BIOCHEMISTRY
including biophysical chemistry & molecular biology

ARTICLE

pubs.acs.org/biochemistry

Mechanistic Studies on Transcriptional Coactivator Protein Arginine Methyltransferase 1

Heather L. Rust,[†,‡] Cecilia I. Zurita-Lopez,[§] Steven Clarke,[§] and Paul R. Thompson*[,†,‡]

[†]Department of Chemistry, The Scripps Research Institute, 130 Scripps Way, Jupiter, Florida 33458, United States

[‡]Department of Chemistry and Biochemistry, University of South Carolina, 631 Sumter Street, Columbia, South Carolina 29208, United States

[§]Department of Chemistry and Biochemistry, University of California, 607 Charles E. Young Drive East, Los Angeles, California 90095, United States

Supporting Information

ABSTRACT: Protein arginine methyltransferases (PRMTs) catalyze the transfer of methyl groups from *S*-adenosylmethionine (SAM) to the guanidinium group of arginine residues in a number of important cell signaling proteins. PRMT1 is the founding member of this family, and its activity appears to be dysregulated in heart disease and cancer. To begin to characterize the catalytic mechanism of this isozyme, we assessed the effects of mutating a number of highly conserved active site residues (i.e., Y39, R54, E100, E144, E153, M155, and H293), which are believed to play key roles in SAM recognition, substrate binding, and catalysis. The results of these studies, as well as pH−rate studies, and the determination of solvent isotope effects (SIEs) indicate that M155 plays a critical role in both SAM binding and the processivity of the reaction but is not responsible for the regiospecific formation of asymmetrically dimethylated arginine (ADMA). Additionally, mutagenesis studies on H293, combined with pH studies and the lack of a normal SIE, do not support a role for this residue as a general base. Furthermore, the lack of a normal SIE with either the wild type or catalytically impaired mutants suggests that general acid/base catalysis is not important for promoting methyl transfer. This result, combined with the fact that the E144A/E153A double mutant retains considerably more activity then the single mutants alone, suggests that the PRMT1-catalyzed reaction is primarily driven by bringing the substrate guanidinium into the proximity of the *S*-methyl group of SAM and that the prior deprotonation of the substrate guanidinium is not required for methyl transfer.

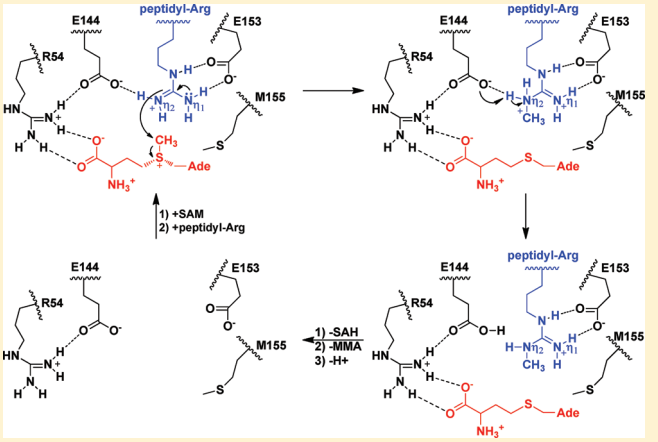

Post-translational modifications of proteins are well-known for the variety of roles they play in controlling cellular function. One specific modification, the methylation of arginine residues, which occurs on numerous proteins (e.g., histones H3 and H4, p53, and p300), is known to modulate a number of cell signaling pathways, including gene transcription, RNA splicing, signal transduction, cell growth, and proliferation (reviewed in refs 1−6). Arginine methylation is catalyzed by the protein arginine methyltransferases (PRMTs), a family of enzymes that catalyze the transfer of a methyl group from *S*-adenosylmethionine (SAM) to the guanidinium moiety of arginine residues in proteins, but not free arginine. This reaction first produces an ω-monomethylarginine residue (ω-MMA), which can then be further methylated to produce either an asymmetrically dimethylated arginine residue (ADMA) or a symmetrically dimethylated arginine (SDMA) residue (Figure 1). In humans, there are nine PRMT family members; PRMT1, -2, -3, -4, -6, and -8 are type I PRMTs that produce ADMA, whereas PRMT5 is a definitive type II PRMT and produces SDMA.[6] Note that the modified arginine products of PRMT7 remain to be clearly established[6] and that enzymatic activity has yet to be demonstrated for PRMT9 (4q31).[6]

All PRMTs possess a highly conserved ∼310-amino acid catalytic core that is responsible for methyltransferase activity. This core consists of a SAM binding domain that contains a Rossmann-type fold typical of class I methyltransferases, a unique β-barrel domain, and a dimerization arm. All family members also possess an N-terminal extension, and several also contain C-terminal extensions.[1−6] PRMT1 is an ∼42 kDa, 353-residue protein that is responsible for ∼85% of in vivo PRMT activity.[5,7]

Received: December 20, 2010
Revised: March 18, 2011
Published: March 21, 2011

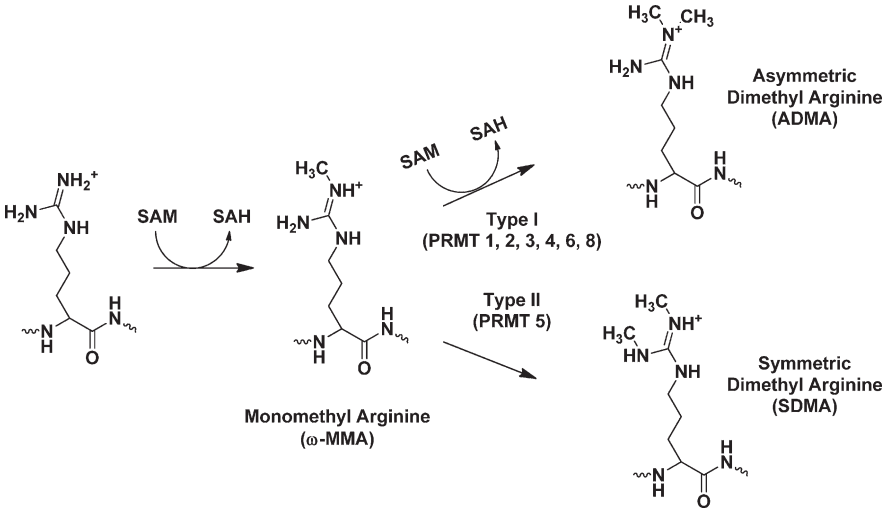

Figure 1. PRMT-catalyzed reactions. PRMTs catalyze the transfer of a methyl group from *S*-adenosylmethionine (SAM) to the guanidinium group of an arginine residue. Type I PRMTs produce asymmetric dimethylarginine (ADMA), and type II PRMTs produce symmetric dimethylarginine (SDMA) via an ω-monomethylated (ω-MMA) intermediate.

This isozyme is located in both the nucleus and the cytoplasm[8] and is active as a head-to-tail dimer, which is formed by the interaction of the dimerization arm of one monomer with the SAM binding domain of another monomer.[9]

Given the links between dysregulated PRMT1 activity and cancer and heart disease,[10−12] we initiated kinetic and mechanistic studies on PRMT1 to aid our efforts to develop inhibitors targeting this isozyme.[13−16] Previously, we demonstrated that PRMT1 preferentially methylates a 21-residue peptide based on the N-terminus of histone H4 with kinetics comparable to those of the parent protein.[13] Additionally, these studies demonstrated that positively charged residues present in the C-terminus of this peptide, which is denoted AcH4−21, are critical for the high rates of catalysis observed with this substrate. We further demonstrated that PRMT1 catalyzes the methylation of the AcH4−21 substrate in a partially processive manner; i.e., PRMT1 can rebind SAM and subsequently produce ADMA before the first methylation product, ω-MMA, is released.[13] Because ADMA formation is not obligatory, we have suggested that PRMT1 displays partial processivity. The partially processive nature of this reaction is entirely consistent with the fact that PRMT1 uses a rapid equilibrium random kinetic mechanism with "dead-end" E· SAM·ω-MMA and E·AcH4−21·SAH complexes, where the E·SAM·ω-MMA complex can undergo a second methyl transfer reaction to produce ADMA.[17]

To follow up on these studies and provide a mechanistic basis for the methylation of an arginine residue, which is arguably a weak nucleophile, we examined the structure of PRMT1 bound to SAH.[9] On the basis of this structure, there are a number of highly conserved active site residues that likely play key roles in SAM recognition, substrate binding, and catalysis (Figure 2A). For example, in PRMT1, it has been suggested that R54 and E100 are involved in SAM binding by forming hydrogen bonds and electrostatic interactions with the carboxylate group and ribose moiety of SAM, respectively.[9,18] The R54 residue also likely forms a hydrogen bond with the side chain of E144 to orient the γ-carboxylate of this residue for optimal electrostatic and hydrogen bonding interactions with N_{η_2} of a substrate arginine residue. This interaction likely helps position N_{η_2} for attack on the methyl group of SAM. The γ-carboxylate of E153 also likely contributes to the alignment of the substrate guanidinium via electrostatic interactions and two hydrogen bonds with N_{η_1} and N_{δ},[9,18] although it should be noted that, in structures of PRMT1, the position of this residue does not appear to be catalytically competent as it is "flipped" out of the active site.[9]

Examination of the crystal structure of CARM1 also identified Y154, a conserved tyrosine residue that corresponds to Y39 in PRMT1, as potentially playing a role in PRMT catalysis. Although Y39 is not visible in the crystal structure of PRMT1, the side chain phenol of this residue forms the top of the SAM binding pocket and is likely important for cofactor binding. Additionally, on the basis of the CARM1 structure, the phenol appears to interact with E153 (PRMT1 numbering) and helps orient this residue and, as a consequence, the substrate guanidinium to promote catalysis.[19,20] The backbone carbonyl oxygen of Y154 in CARM1 also appears to be important for CARM1 catalysis via the formation of a hydrogen bond with the hydroxyl group of a conserved serine residue, S217 in CARM1 (S102 in PRMT1); this latter interaction likely helps to orient the Y154 phenol for interaction with E267. It has been hypothesized that S217 and Y154 play an important role in regulating CARM1 activity.[21] This is the case because S217 can be phosphorylated in vivo, and this modification is associated with a loss of CARM1 activity; phosphorylation presumably disrupts the hydrogen bond between the S217 hydroxyl and the backbone carbonyl of Y154, leading to a loss of affinity for SAM and an inability to properly position the Y154 phenol.[21] Because residues from the N-terminal tail are absent in the holo structure of PRMT1 and an apo structure does not exist, it is unclear whether this interaction occurs in PRMT1.

Also present in the active site is M155. Although this residue is not thought to play a direct role in rate acceleration, it has been suggested[22] that M155 is responsible for the formation of ADMA as the end product of dimethylation, as opposed to SDMA, because of steric hindrance that would prevent the transfer of a methyl group to N_{η_1} after methylation of N_{η_2}.[18,22] This hypothesis is supported by the fact that PRMT5, a type II PRMT, has a serine residue at this position that presumably creates a more open pocket that allows symmetric dimethylation.[22]

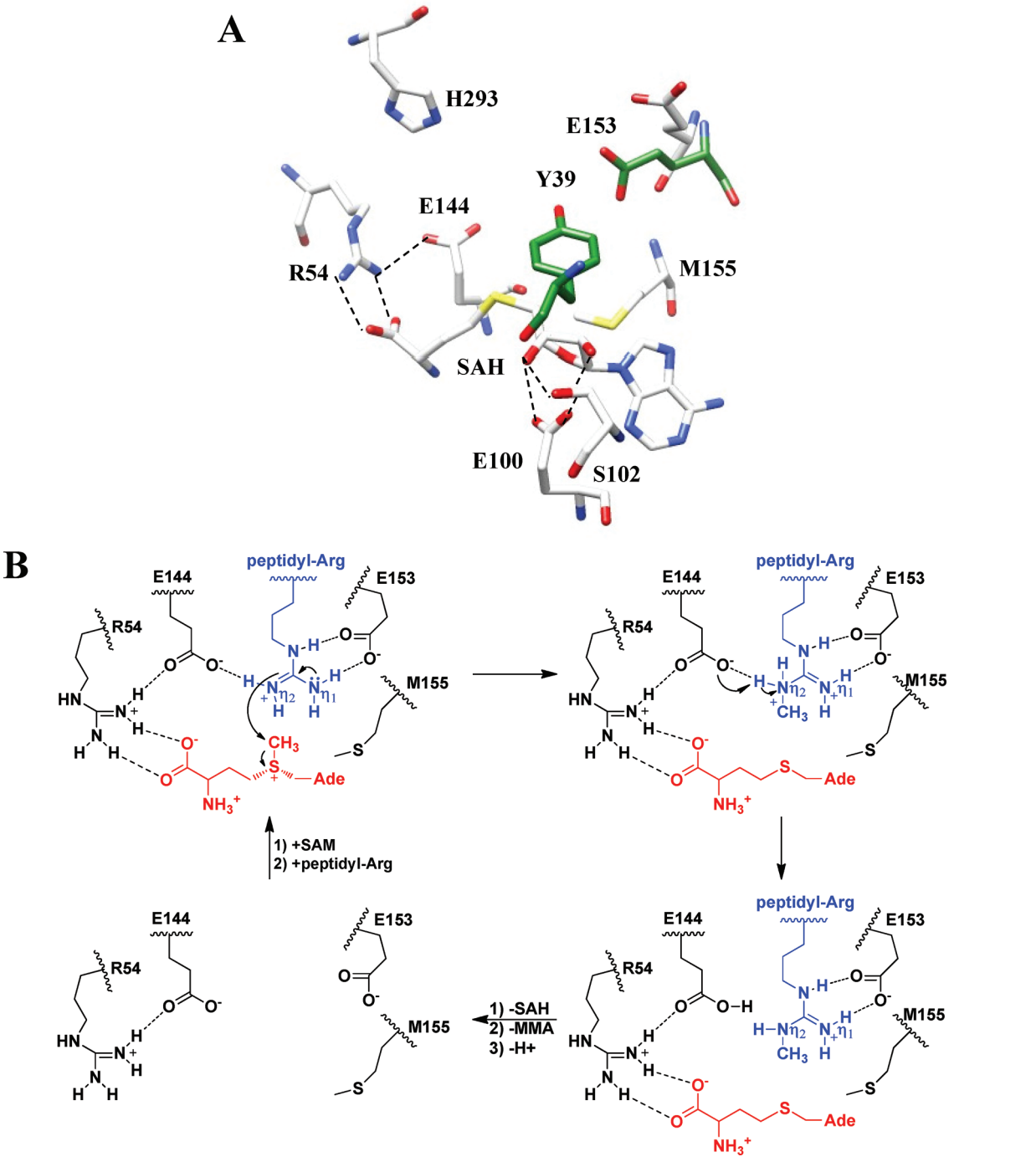

Figure 2. Active site and proposed catalytic mechanism of PRMT1. (A) Structure of PRMT1 (white) highlighting key residues in the active site believed to play roles in substrate binding and/or catalysis. Note that the PRMT1 structure is overlaid with PRMT3 (green) because the electron density of Y39 is not present in the crystal structure of PRMT1 and the positioning of E153 in PRMT1 is different from that in PRMT3, which is likely due to the crystallization conditions. This figure was prepared with UCSF Chimera using the coordinates from PRMT1 (PDB entry 1ORI) and PRMT3 (PDB entry 1F3L). (B) Proposed catalytic mechanism of PRMT1. The proposed mechanism of catalysis involves three conserved active site residues. It has been suggested that R54 and E144 help position N_{η_2} of a substrate Arg residue for attack on the methyl group of SAM. E153 plays a role in positioning the Arg residue as well as initiating an electron rearrangement that results in the formation of a more nucleophilic guanidinium moiety. Methyl transfer results in the formation of a dication intermediate that then undergoes the loss of a proton to form the first methylation product, ω-MMA. A second round of methylation occurs via the same mechanism to form the final product, ADMA.

Given that the guanidinium group is a relatively weak nucleophile, it has been suggested that its interaction with E153 causes a redistribution of electrons that activates N_{η_2} for an S_N2-type nucleophilic attack on the methyl group of SAM (Figure 2B).[18] This attack potentially results in the formation of a dication intermediate that undergoes the loss of a proton to possibly E144 or via a proton wire to H293. However, because the formation of a dication intermediate is somewhat unfavorable, it has been

dx.doi.org/10.1021/bi102022e |*Biochemistry* 2011, 50, 3332–3345

suggested that PRMT1 uses a stepwise or concerted mechanism in which the proton is removed prior to or simultaneously with methyl transfer.[18]

To confirm the assumed roles of the aforementioned residues and to begin to validate the proposed mechanism, we initiated studies to characterize the catalytic mechanism of PRMT1. Herein we describe those efforts. Specifically, we report the results of site-directed mutagenesis of a number of highly conserved active site residues (i.e., Y39, R54, E100, E144, E153, M155, and H293), which are believed to play key roles in SAM recognition, substrate binding, and catalysis, as well as pH−rate profiles, processivity studies, and the determination of solvent isotope effects (SIEs). In particular, we demonstrate that while E100 is not important for SAM binding, M155 plays a critical role in this process, as well as the processivity of the enzyme; however, M155 is not responsible for the regiospecific formation of ADMA. Additionally, while R54 is not important for SAM binding, this residue likely forms a hydrogen bond with E144, and this interaction appears to be important for orienting the substrate guanidinium for nucleophilic attack on the *S*-methyl group of SAM. While our data suggest that the charge of E144 is not important for catalysis, the charge and position of E153 are critical. The Y39 phenol also plays an important role in rate enhancement, likely via its ability to form a hydrogen bond with the E153 carboxylate or the substrate guanidinium. Additionally, mutagenesis studies on H293, combined with the lack of a normal SIE, do not support a role for this residue as a general base. Furthermore, the lack of a normal SIE with either the wild type (WT) or catalytically impaired mutants suggests that general acid/base catalysis is not important for promoting methyl transfer. This result, combined with the fact that the E144A/E153A double mutant retains considerably more activity then the single mutants alone, suggests that the PRMT1-catalyzed reaction is primarily driven by proximity effects and that the prior deprotonation of the substrate guanidinium is not required for methyl transfer.

MATERIALS AND METHODS

Chemicals. Sodium dodecyl sulfate (SDS), tris(hydroxymethyl) aminomethane (TRIS), tetramethylethylenediamine, acrylamide, and ammonium persulfate were purchased from Bio-Rad (Hercules, CA). 4-(2-Hydroxyethyl)-1-piperazineethanesulfonic acid (HEPES), Tricine, and dithiothreitol (DTT) were purchased from RPI (Mt. Prospect, IL). Acetonitrile and methanol were purchased from Fisher Scientific (Pittsburgh, PA). Sodium chloride and dimethylformamide (DMF) were purchased from Alfa Aesar (Ward Hill, MA). Piperidine was purchased from Sigma-Aldrich (St. Louis, MO). Fmoc-protected amino acids, (ethylenedinitrilo)tetraacetic acid (EDTA), and trifluoroacetic acid (TFA) were purchased from EMD (Gibbstown, NJ). ^{14}C-labeled SAM was purchased from Perkin-Elmer and ^{14}C-labeled BSA from Sigma-Aldrich. Mutagenic primers were purchased from IDT Inc. (Coralville, IA). The purification of PRMT1 has been described previously.[13]

Site-Directed Mutagenesis. PRMT1 mutants were generated using the QuikChange site-directed mutagenesis kit (Stratagene). The sequences of the mutagenic primers can be found in Table S1 of the Supporting Information. The full open reading frame was sequenced for each mutant to ensure that only the desired mutation had been incorporated. DNA that contained the desired mutation was then transformed into *Escherichia coli* BL21(DE3) cells and purified using our established protocol for WT PRMT1.[13]

Table 1. Peptide Sequences

peptide	sequence
AcH4−21	1-Ac-SGRGKGGKGLGKGGAKRHRKV
RGG3	GGRGGFGGRGGFGGRGGFG

Synthesis of Peptides. AcH4−21 and RGG3 peptides were synthesized as previously described on a Rainin PS3 automatic peptide synthesizer using Fmoc chemistry on a Wang resin.[13] The sequences of these peptides can be found in Table 1. The peptides were cleaved from the resin with 95% TFA, 2.5% triisopropylsilane, and 2.5% water and then precipitated with diethyl ether. Peptides were purified by reverse phase HPLC with a mobile phase of water and 0.05% TFA and eluted with acetonitrile and 0.05% TFA. The masses were determined using a Bruker Ultraflex II MALDI-TOF mass spectrometer.

Gel-Based Activity Assay. A previously described gel-based assay was used to determine the steady state kinetic parameters of WT and PRMT1 mutants.[13] Assays were performed in a reaction mixture of 50 mM HEPES (pH 8.0), 1 mM EDTA, 50 mM NaCl, 0.5 mM dithiothreitol, 15 μM ^{14}C-labeled SAM, and a varying final concentration of AcH4−21 (0−1000 μM). Reaction mixtures were preincubated at 37 °C for 10 min. WT PRMT1, or a PRMT1 mutant, was then added, and the reaction was quenched after 15 min. For the assays with a varying final SAM concentration (0−39.7 μM), the same reaction mixture was used except the concentration of AcH4−21 was held constant at 100 μM. Each assay was conducted in duplicate, and the standard deviation of the duplicate raw data values agreed within ≤20%. GraFit version 5.0.11[23] was used to fit the data to eq 1 or 2 if substrate inhibition was observed

$$v = V_{max}[S]/(K_m + [S]) \quad (1)$$

$$v = V_{max}[S]/[(K_m + [S])(1 + [S]/K_i)] \quad (2)$$

MALDI-MS-Based Activity Assay. A previously described matrix-assisted laser desorption ionization (MALDI) MS-based assay was used to determine the processivity of WT and select PRMT1 mutants.[13] Briefly, assays were performed in a reaction mixture of 50 mM HEPES (pH 8.0), 1 mM EDTA, 50 mM NaCl, 500 μM SAM, and 20 μM AcH4−21. Reaction mixtures were then preincubated at 37 °C for 10 min. WT PRMT1 or a PRMT1 mutant was then added, and the reaction was quenched with 3 μL of 50% TFA in ddH_2O after the appropriate time period. Spectra were recorded on a Bruker Ultraflex II MALDI-TOF MS or Applied Biosystems 4800 Plus MALDI TOF/TOF MS instrument and analyzed using Flex Analysis. The percent turnover was determined by dividing the intensity of the modified peptide by the sum of the intensities of the unmodified and modified substrates times 100%.

Chemical Analysis of Methylation Products. A reaction mixture of 10 μg of GST-GAR and 1.4 μM [^{3}H]SAM in 50 mM HEPES (pH 7.5) was incubated with 2 μg of WT PRMT1 or a PRMT1 mutant for 2 h at 37 °C. The products were then precipitated with an equal volume of 50% trichloroacetic acid, washed with acetone, and hydrolyzed for 20 h at 110 °C in 6 M HCl. The hydrolysate was dried and mixed with standards of ADMA, SDMA, and ω-MMA before being fractionated on a high-resolution cation exchange column as described previously.[24] One-tenth of the fractions were used for ninhydrin analysis of the standards, and nine-tenths were counted.

Partial Proteolysis. Partial proteolysis assays were performed in a reaction mixture of 50 mM HEPES (pH 8.0), 1 mM EDTA, 50 mM NaCl, and 0.5 mM dithiothreitol in the absence or presence of 0.5 mM SAH and 0.75 μg/mL subtilisin on ice. WT PRMT1, or a PRMT1 mutant, was then added, and the reaction was quenched after 60 min with 5 mM phenylmethanesulfonyl fluoride. Protein fragments were separated by 12% sodium dodecyl sulfate−polyacrylamide gel electrophoresis and visualized with Coomassie Brilliant Blue.

pH Profile. The steady state kinetic parameters for the WT enzyme as well as the Y39F and H293A mutants were determined over a pH range of 6.0−9.25 using the gel-based activity assay described above. Assays were performed in a reaction mixture of 50 mM Bis-Tris (6.0−7.0), 50 mM HEPES (7.0−8.5), 50 mM Tricine (8.5−9.0), or CHES (8.75−9.25), 1 mM EDTA, 50 mM NaCl, and 0.5 mM dithiothreitol, with constant and varying final concentrations of [^{14}C]SAM (0−41 μM) and RGG3 (0−1000 μM). Each assay was conducted in duplicate, and the standard deviation of the duplicate measurements agreed within ≤20%. Note that, to make certain that the variances in kinetic parameters were not the result of a buffer effect, we utilized an overlapping buffer method. The kinetic parameters for the overlapping buffers were similar, and thus, the average was used. In addition, time course assays were performed at each pH to demonstrate that activity was not lost over time. GraFit version 5.0.11[23] was used to fit the data to eq 3 or 4

$$y = (\mathrm{Lim1} + \mathrm{Lim2} \times 10^{\mathrm{pH}-\mathrm{p}K_{a1}})/(10^{\mathrm{pH}-\mathrm{p}K_{a1}} + 1) - [(\mathrm{Lim2} - \mathrm{Lim3}) \times 10^{\mathrm{pH}-\mathrm{p}K_{a2}}]/(10^{\mathrm{pH}-\mathrm{p}K_{a2}} + 1) \quad (3)$$

$$y = (\mathrm{Lim1} + \mathrm{Lim2} + 10^{\mathrm{pH}-\mathrm{p}K_{a1}})/(10^{\mathrm{pH}-\mathrm{p}K_{a1}} + 1) \quad (4)$$

For eqs 3 and 4, Lim1 corresponds to the activity measured at low pH and Lim2 corresponds to the maximal activity measured at the optimal pH, and for eq 3, Lim3 is equal to the activity measured at high pH.

Solvent Isotope Effect. SIEs were investigated by determining the steady state kinetic parameters for the WT enzyme using the gel-based activity assay described above. The reaction mixture consisted of 50 mM HEPES (pH 8.0), 1 mM EDTA, 50 mM NaCl, 0.5 mM dithiothreitol, 15 μM ^{14}C-labeled SAM, and a varying final concentration of AcH4−21 (0−1000 μM) in >92% D_2O. The assay was conducted in duplicate, and the standard deviation of the duplicate measurements agreed within ≤20%. GraFit version 5.0.11[23] was used to fit the data to eq 1.

SAH Inhibition Studies. The inhibition constants for SAH were determined for the WT and mutant enzymes using the gel-based activity assay described above. The reaction mixture consisted of 50 mM HEPES (pH 8.0), 1 mM EDTA, 50 mM NaCl, 0.5 mM dithiothreitol, 15 μM ^{14}C-labeled SAM, 100 μM AcH4−21, and a varying final concentration of SAH (0−500 μM). The assay was conducted in duplicate, and the standard deviation of the duplicate measurements agreed within ≤20%. GraFit version 5.0.11[23] was used to fit the data to a Dixon plot of $1/v$ versus SAH concentration. K_i was determined using eq 5

$$\mathrm{slope} = K_m/(V_{max}K_i[S]) \quad (5)$$

pK_a Calculations. The structure of PRMT1 (PDB entry 1ORI) was rebuilt using Amber topology parameters and hydrogen atoms added to the structure. Atom partial charges and atomic radii were assigned on the basis of the Amber99 force field using AMBER.[25] pK_a values were computed taking into account desolvation effects and intraprotein interactions, including the proximity of neighboring functional groups.[26]

RESULTS AND DISCUSSION

Mutagenesis Studies of Proposed Catalytic Residues. To begin to investigate the catalytic mechanism of PRMT1, we used site-directed mutagenesis to probe the roles of Y39, R54, E100, S102, E144, E153, M155, and H293. The mutant enzymes were purified and characterized according to described procedures.[13] The kinetic parameters of each mutant were determined for the AcH4−21 peptide as well as SAM (Tables 2 and 3); AcH4−21 is a 21-amino acid peptide substrate whose sequence is based on the N-terminus of histone H4 (Table 1). Note that, like other systems,[27,28] partial proteolysis studies were performed to ensure that the loss of activity associated with a particular mutation was not due to a gross structural perturbation (Figure S1 of the Supporting Information).

SAM Binding Mutants. *R54 Mutants.* R54 forms hydrogen bonds and/or electrostatic interactions with E144, one of the two key glutamate residues, and presumably orients this residue for the productive recognition of the substrate guanidinium. Additionally, both N_{η_1} and N_{η_2} of this residue interact with the carboxylate group on the methionine portion of SAM, which suggests that this residue could play a key role in SAM binding (Figure 2B). Consistent with this prediction is the 42-fold decrease in the k_{cat}/K_m value observed for SAM with the R54K mutant. However, the effect on k_{cat}/K_m is primarily driven by a decrease in k_{cat} and not K_m, suggesting that the lack of a more dramatic effect on the SAM K_m reflects the multistep nature of the reaction, where K_d is not equal to K_m; k_{cat}/K_m represents all steps up to and including the first irreversible step of the reaction. To evaluate whether this was indeed the case, we determined the dissociation constants, i.e., K_i, for binding of SAH to both the WT and R54A enzymes; SAH was used for these experiments as a proxy for SAM to more accurately gauge the effects of a particular mutation on SAM binding. The results of these studies confirm that R54 is not critical for SAM binding, as evidenced by the fact that the K_i for SAH is similar to that obtained for the WT enzyme (Table 4).

With respect to the peptide substrate, large changes in both $k_{cat(app)}$ (42- and 7.7-fold) and $k_{cat(app)}/K_m$ (32- and 32-fold) were observed for both the R54K and R54A mutants, respectively. Although these effects are at least partially related to our inability to completely saturate the enzyme with SAM in our radioactive methyltransferase assay, which is why the term $k_{cat(app)}$ is used, their magnitude, particularly on $k_{cat(app)}$, is consistent with a role for this residue in orienting the substrate guanidinium via E144 for nucleophilic attack on the methyl group of SAM. Consistent with this notion is the fact that the k_{cat} values obtained with SAM, where the peptide substrate is saturating, are decreased by a similar order of magnitude.

E100 Mutants. E100 forms hydrogen bonds with the ribose moiety of SAM and thus would be expected to play an important role in SAM binding. Three mutants, i.e., the E100D, E100Q, and E100A mutants, were made to confirm this hypothesis. With respect to the kinetic parameters determined for SAM, there is an only very small effect on k_{cat}/K_m. For example, the complete removal of the E100 carboxylate, which occurs in the E100A mutant, decreases k_{cat}/K_m by only 3.2-fold. The K_i for

Table 2. Kinetic Parameters of PRMT1 Mutants for the AcH4−21 Peptide Substrate

	K_m (μM)	*x*-fold	$k_{cat(app)}$ (min^{-1})	*x*-fold	$k_{cat(app)}/K_m$ (M^{-1} min^{-1})	*x*-fold
WT[a]	1.1 ± 0.5	–	$4.6 \times 10^{-1} \pm 2 \times 10^{-2}$	–	4.1×10^5	–
Y39F[a]	2.0 ± 0.7	1.8	$4.2 \times 10^{-2} \pm 2 \times 10^{-3}$	11	2.1×10^4	20
R54K[a]	0.8 ± 0.6	0.7	$1.09 \times 10^{-2} \pm 4 \times 10^{-4}$	42	1.3×10^4	32
R54A[a]	5 ± 1	4.5	$6.0 \times 10^{-2} \pm 3 \times 10^{-3}$	7.7	1.3×10^4	32
E100D[a]	5 ± 1	4.5	$3.6 \times 10^{-1} \pm 1 \times 10^{-2}$	1.3	7.6×10^4	5.4
E100Q[a]	6 ± 2	5.5	$2.5 \times 10^{-1} \pm 1 \times 10^{-2}$	1.8	4.5×10^4	9.1
E100A[a]	2.6 ± 0.9	2.4	$1.85 \times 10^{-1} \pm 8 \times 10^{-3}$	2.5	7.2×10^4	5.7
S102E[a]	5 ± 1	4.5	$5.7 \times 10^{-1} \pm 2 \times 10^{-2}$	0.8	1.1×10^5	3.7
S102A[a]	6 ± 1	5.5	$6.3 \times 10^{-1} \pm 2 \times 10^{-2}$	0.7	1.1×10^5	3.7
E144D[a]	1.7 ± 0.4	1.5	$2.2 \times 10^{-1} \pm 1 \times 10^{-2}$	2.0	1.3×10^5	3.2
E144Q[a]	2.0 ± 0.6	1.8	$1.3 \times 10^{-1} \pm 4 \times 10^{-3}$	3.5	6.7×10^4	6.1
E144A[a]	0.3 ± 0.2	0.3	$9.5 \times 10^{-3} \pm 2 \times 10^{-4}$	50	3×10^4	14
E153D[a]	3.1 ± 0.5	2.8	$2.65 \times 10^{-2} \pm 5 \times 10^{-4}$	17	8.6×10^3	50
E153Q[a]	2.0 ± 0.8	1.8	$7.7 \times 10^{-3} \pm 3 \times 10^{-4}$	60	3.8×10^3	110
E153A[a]	1.8 ± 0.6	1.6	$3.8 \times 10^{-3} \pm 1 \times 10^{-4}$	121	2.2×10^3	190
E144A/E153A[a]	3.0 ± 0.7	2.7	$1.32 \times 10^{-1} \pm 4 \times 10^{-3}$	3.5	4.4×10^4	9.3
M155L[a]	0.6 ± 0.4	0.5	$1.73 \times 10^{-1} \pm 5 \times 10^{-3}$	2.7	3×10^5	1.4
M155A[b]	1.8 ± 0.5	1.6	$4.6 \times 10^{-2} \pm 1 \times 10^{-3}$	10	2.6×10^4	16
H293Q[a]	2 ± 2	1.8	$7.6 \times 10^{-3} \pm 6 \times 10^{-4}$	61	3.7×10^3	110
H293A[a]	11.1 ± 0.6	10	$1.81 \times 10^{-2} \pm 2 \times 10^{-4}$	25	1.6×10^3	256

[a] At 15 μM SAM. [b] At 30 μM SAM.

Table 3. Kinetic Parameters of PRMT1 Mutants for SAM

	K_m (μM)	*x*-fold	k_{cat} (min^{-1})	*x*-fold	k_{cat}/K_m (M^{-1} min^{-1})	*x*-fold
WT[a]	6 ± 1	–	$5.8 \times 10^{-1} \pm 3 \times 10^{-2}$	–	1×10^5	–
Y39F[a]	14 ± 3	2.3	$7.0 \times 10^{-2} \pm 5 \times 10^{-3}$	8.3	5.1×10^3	20
R54K[a]	14 ± 1	2.3	$3.3 \times 10^{-2} \pm 1 \times 10^{-3}$	18	2.4×10^3	42
R54A[a]	10 ± 1	1.7	$9.5 \times 10^{-2} \pm 4 \times 10^{-3}$	6.1	9.1×10^3	11
E100D[a]	6 ± 2	1.0	$4.8 \times 10^{-1} \pm 5 \times 10^{-2}$	1.2	7.8×10^4	1.3
E100Q[a]	7 ± 2	1.2	$2.8 \times 10^{-1} \pm 2 \times 10^{-2}$	2.1	3.8×10^4	2.6
E100A[a]	5 ± 2	0.8	$1.6 \times 10^{-1} \pm 2 \times 10^{-2}$	3.6	3.1×10^4	3.2
S102E[a]	5.1 ± 0.7	0.9	$5.1 \times 10^{-1} \pm 2 \times 10^{-2}$	1.1	9.9×10^4	1.0
S102A[a]	5.6 ± 0.6	0.9	$5.2 \times 10^{-1} \pm 2 \times 10^{-2}$	1.1	8.8×10^4	1.1
E144D[a]	4.0 ± 0.9	0.7	$2.7 \times 10^{-1} \pm 2 \times 10^{-2}$	2.1	6.8×10^4	1.5
E144Q[a]	8.3 ± 0.9	1.4	$1.60 \times 10^{-1} \pm 7 \times 10^{-3}$	3.6	1.9×10^4	5.3
E144A[a]	3.1 ± 0.6	0.5	$1.05 \times 10^{-2} \pm 4 \times 10^{-4}$	55	3.4×10^3	29
E153D[a]	5 ± 1	0.8	$2.8 \times 10^{-2} \pm 2 \times 10^{-3}$	21	5.8×10^3	17
E153Q[a]	17 ± 4	2.8	$1.9 \times 10^{-2} \pm 2 \times 10^{-3}$	31	1.1×10^3	91
E153A[a]	9 ± 3	1.5	$4.1 \times 10^{-3} \pm 4 \times 10^{-4}$	141	4×10^2	250
E144A/E153A[a]	10 ± 2	1.7	$1.06 \times 10^{-1} \pm 6 \times 10^{-3}$	5.5	1.1×10^4	9.1
M155L[a]	10 ± 2	1.7	$1.00 \times 10^{-1} \pm 8 \times 10^{-3}$	5.8	1×10^4	10
M155A[a]	110 ± 21	18	$2.9 \times 10^{-1} \pm 4 \times 10^{-2}$	2.0	2.8×10^3	36
H293Q[a]	17 ± 6	2.8	$1.4 \times 10^{-2} \pm 2 \times 10^{-3}$	41	8×10^2	125
H293A[a]	37 ± 2	6.2	$5.6 \times 10^{-2} \pm 1 \times 10^{-3}$	10	2×10^3	50

[a] At 100 μM AcH4−21.

SAH with this mutant is similarly unaffected, quite clearly demonstrating that this residue is not important for SAM binding or catalysis. This result is especially surprising when one considers that the distances between the ribose hydroxyls and the α-carboxylate of E100 in the PRMT1·SAH complex are only 2.6−2.7 Å, which are distances typically associated with relatively strong hydrogen bonds. Although the observed interactions may be an artifact of the crystallization conditions (the enzyme was crystallized at pH ~4.7, which would favor protonation of E100 and potentially promote hydrogen bond formation), similar distances and orientations are observed in the crystal structures of the PRMT3·SAH and CARM1·SAH complexes that were crystallized at pH 6.3 and 7, respectively.[18,29] Thus, such an explanation is intellectually unsatisfying. Nevertheless, these results

dx.doi.org/10.1021/bi102022e |*Biochemistry* 2011, 50, 3332–3345

Table 4. SAH Inhibition Studies

	K_i (μM)
WT	1.28 ± 0.06
Y39F	26 ± 1
R54A	1.8 ± 0.2
E100A	1.9 ± 0.1
M155A	34 ± 6

are consistent with the fact that methylthioadenosine is a relatively poor PRMT1 inhibitor.[13]

With respect to the kinetic parameters determined for the AcH4−21 peptide, the effects, while still small, are significantly larger than those observed with SAM. For example, the decreases in $k_{cat(app)}/K_m$ for the E100D, E100Q, and E100A mutants are 5.4-, 9.1-, and 5.7-fold, respectively. As the effects are largely driven by an increase in K_m, these results suggest that an interplay exists between the binding of both substrates or, alternatively, a change in the kinetic mechanism.

M155 Mutants. To probe the importance of M155, we created the M155L and M155A mutants. With respect to the peptide substrate, the kinetic parameters for the M155L mutant were similar to those obtained for the WT enzyme; the $k_{cat(app)}$ and $k_{cat(app)}/K_m$ values were only decreased by 2.7- and 1.4-fold, respectively. In contrast to these relatively minor effects, 5.8- and 10-fold decreases in k_{cat} and k_{cat}/K_m, respectively, were observed when SAM was tested as the varied substrate. These effects represent an inability to properly position the *S*-methyl group of SAM or, alternatively, an effect on SAM binding. Given that M155 forms the bottom of the adenine portion of the SAM binding pocket, these results are most consistent with the latter possibility because the structural differences between a leucine and a methionine would be expected to alter SAM binding. Similar effects on SAM binding are observed with the M155A mutant, where the K_m for SAM was increased by 18-fold and the k_{cat}/K_m was decreased by 36-fold. Further confirming that this residue is important for SAM binding is the fact that the K_i for SAH is increased by 27-fold relative to that of WT. The large changes in K_i, K_m, and k_{cat}/K_m likely reflect a loss of steric constraint within the SAM binding pocket, which disfavors the binding of SAM in an orientation that is productive for catalysis. With respect to the peptide substrate, 10- and 16-fold reductions in $k_{cat(app)}$ and $k_{cat(app)}/K_m$, respectively, were observed. These effects are most likely due to our inability to completely saturate the enzyme with SAM in our radioactive methyltransferase assay.

Role of M155 in ADMA Formation. Given the postulated role of M155 in directing the formation of ADMA, as opposed to SDMA,[18,22] we also investigated the contribution of this residue to the regiospecific dimethylation of a substrate arginine residue. For these studies, the M155A mutant was utilized because we hypothesized that this mutation would relieve the steric constraint imposed by the methionine and thereby open up the pocket and allow for SDMA formation. To investigate this possibility, the M155A mutation, along with the WT control, was used to catalyze the [^{3}H]SAM-dependent methylation of GST-GAR, a fusion protein that links GST to the N-terminus of human fibrilarin (Figure 3). Subsequently, the reaction mixture was hydrolyzed in 6 M HCl at 110 °C, and the levels of ω-MMA, SDMA, and ADMA formed were quantified by high-resolution cation exchange chromatography. The results of these experiments indicate that the M155A mutant catalyzes the exclusive formation of ω-MMA and ADMA. Thus, despite the fact that this mutation relieves the steric constraint thought to prevent SDMA formation, our results indicate M155 is not responsible for the formation of ADMA over SDMA.

Nevertheless, given that the mutation of this residue strongly impacts the kinetics of the PRMT1-catalyzed reaction, particularly with respect to the K_m for SAM, we reasoned that it may play a role in the processivity of ADMA formation. To investigate this possibility, we utilized a previously established MALDI-MS assay.[13] Consistent with previous results with the WT enzyme, ω-MMA- and ADMA-containing peptides were initially produced in equimolar amounts, followed by a decrease in the levels of ω-MMA (Figure 4A). As described previously, these results are characteristic of an enzyme that has the ability to rebind SAM and subsequently produce ADMA before the first methylation product, ω-MMA, is released.[13] Because ADMA formation is not obligatory, we have suggested that PRMT1 displays partial processivity. With respect to the M155L mutant, similar results were obtained; however, the level of ADMA formed is significantly lower at the early time points (Figure 4B). This result indicates that the M155L mutant is significantly less processive than the WT enzyme. For the M155A mutant, little to no ADMA is formed until the 20 min time point (Figure 4C), which suggests that ω-MMA is released prior to the rebinding of SAM and that this mutant utilizes a distributive mechanism. Note that the concentration of SAM used in these assays was 500 μM; thus, the loss of processivity is not due to a failure to saturate the enzyme with SAM. In total, these results are consistent with M155 playing a key role in SAM binding, as reduced affinity for SAM, which occurs with the M155L and M155A mutants, would be expected to decrease the processivity of the enzyme because, for these mutants, the off rate for the monomethylated peptide is larger than the rate constant for SAM binding.

Catalytic Mutants. *E144 Mutants.* E144 appears to orient N_{η_2} of the substrate guanidinium group to facilitate nucleophilic attack on the *S*-methyl group of SAM. To investigate this role, we created the E144D, E144Q, and E144A mutants. The k_{cat}/K_m values for the E144D mutant were decreased by 3.2- and 1.5-fold for AcH4−21 and SAM, respectively. The ability of aspartate to substitute for the glutamate indicates flexibility within the active site and reveals that positioning of this residue is not critical for catalysis. For the E144Q mutant, the effects on k_{cat}/K_m are slightly larger, with these values decreased 6.1- and 5.3-fold for AcH4−21 and SAM, respectively. These data suggest that the charge of this residue is significantly less important than its ability to hydrogen bond with both the substrate guanidinium and R54, as opposed to modulating the nucleophilicity of that group. Note that the calculated pK_a of the E144 carboxylate is ~2.7; thus, this residue is likely deprotonated in the PRMT1 active site. Nevertheless, this residue is important for catalysis, as illustrated by the 14- and 29-fold decreases in the k_{cat}/K_m values for AcH4−21 and SAM, respectively, for the E144A mutant. Note the effects on k_{cat}/K_m are dominated by a decreased k_{cat}, suggesting that this residue is relatively unimportant for substrate binding. These results are consistent with previous findings from mutagenesis studies that only measured relative rates.[9] In total, the data suggest that the hydrogen bonding characteristics, and to a lesser extent, the charge of E144 are important for orienting the substrate guanidinium for nucleophilic attack on the *S*-methyl group of SAM.

E153 Mutants. The carboxylate group of E153 is thought to play a crucial role in catalysis through its electrostatic and hydrogen bonding interactions with N_{η_1} and N_δ of the substrate

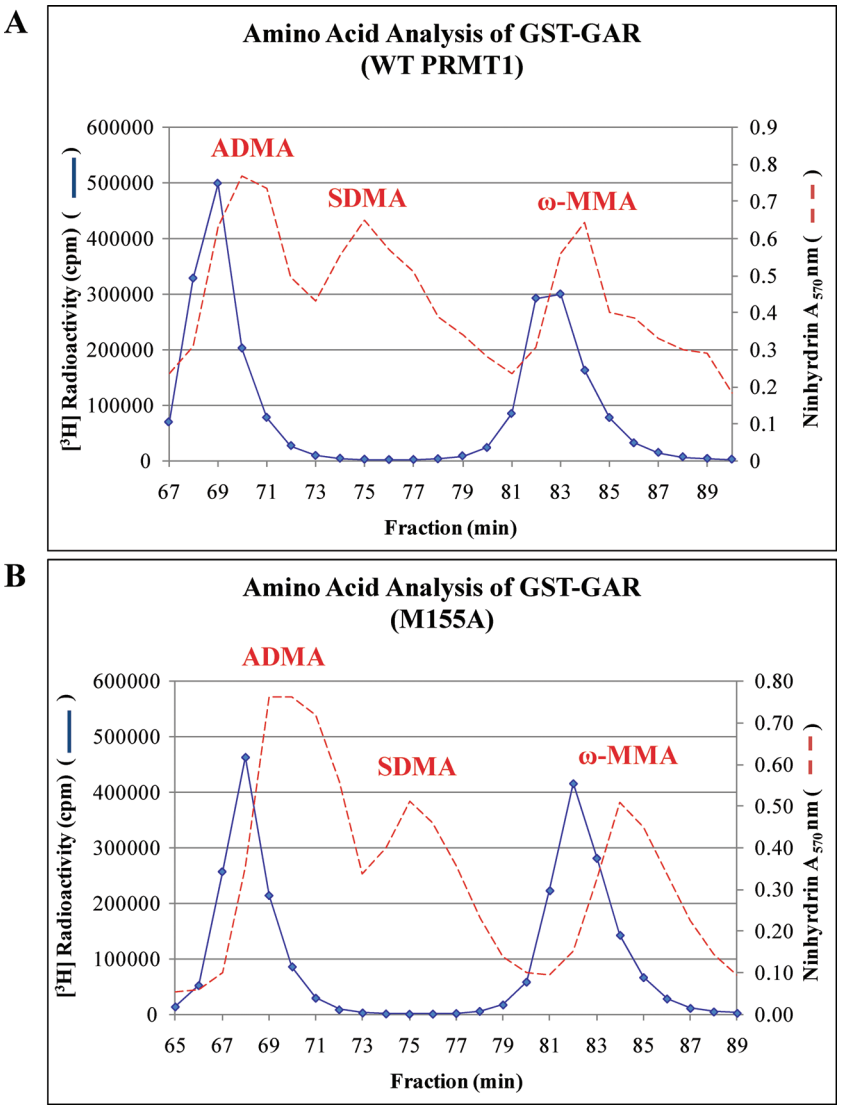

Figure 3. Amino acid analysis of methylation products. (A) WT PRMT1 produces a mixture of ω-MMA and ADMA as products of methylation. (B) The M155A mutant also produces a mixture of ω-MMA and ADMA as products of methylation. In each case, the position of the standards was determined with a ninhydrin assay (dotted lines); the position of the ^{3}H-radiolabeled derivatives by counting (solid lines). The slightly earlier elution position of the [^{3}H]ADMA and [^{3}H]-ω-MMA products compared to the standards is due to the mass and pK_a differences of amino acids with tritium vs hydrogen-containing methyl groups.[24]

guanidinium. To investigate the importance of both the size and charge of this residue, we created the E153D, E153Q, and E153A mutants and determined the kinetic parameters. The results are consistent with this residue playing a key role in catalysis. For example, the k_{cat} values for the E153D, E153Q, and E153A mutants are decreased by 21-, 31-, and 140-fold, respectively. Given that the effects on k_{cat}/K_m mirror the effects on k_{cat}, these data indicate that both the charge and the position of E153 are more important for catalysis than substrate binding. These results are also consistent with previous findings from mutagenesis studies that measured only relative rates.[9] The fact that mutating E153 has a more dramatic effect than mutating E144 is consistent with the notion that this residue plays an important role in redistributing electron density within the guanidinium group to enhance its nucleophilicity.

E144A/E153A Mutant. Given the results obtained for the E144 and E153 single mutants, we expected that the E144A/E153A double mutant would likely yield negligible, if any, activity. However, this was not the case, as k_{cat} is decreased by only 5.5-fold and the k_{cat}/K_m values are decreased by only 9.3- and 9.1-fold for AcH4−21 and SAM, respectively. The more significant effect on the single mutants is most easily explained by the formation of a strong salt bridge to the remaining glutamate. Such an interaction would be expected to decrease activity by altering both the nucleophilicity of the guanidinium and its position such that methyl transfer is suboptimal. The fact that the double mutant retains considerable activity is more difficult to rationalize. However, it is possible that the removal of the two glutamate residues increases the hydrophobicity of the active site, which would be expected to depress the pK_a of the guanidinium and thereby increase its nucleophilicity. Although we cannot rule out such a possibility, the active site possesses a number of other hydrophilic residues in the proximity (e.g., Y39, R54, and H293) that should minimize any change in hydrophobicity. An alternative

dx.doi.org/10.1021/bi102022e |*Biochemistry* 2011, 50, 3332–3345

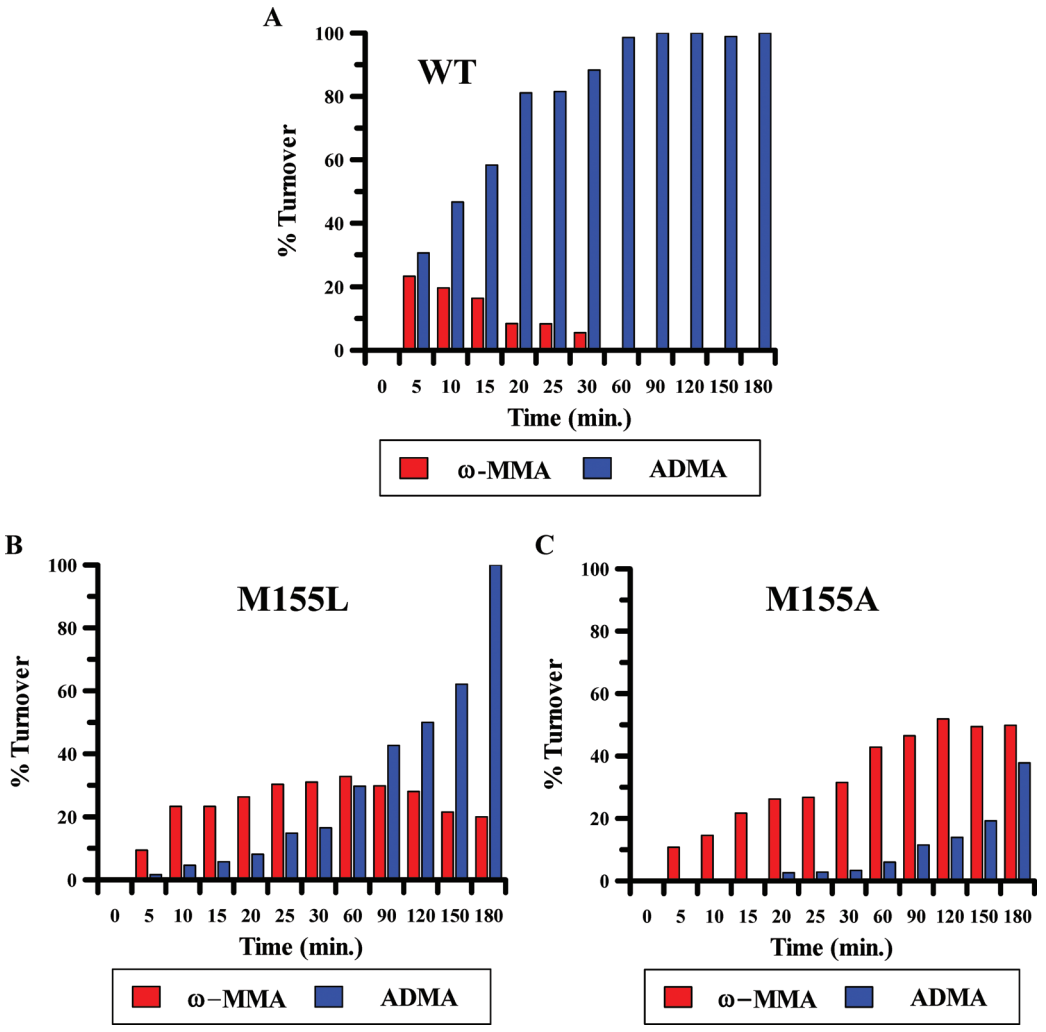

Figure 4. Processivity of WT PRMT1 and M155 mutants. (A) WT PRMT1 uses a partially processive mechanism to catalyze the formation of ADMA. (B) The M155L mutant uses a partially processive mechanism; however, formation of ADMA is slower than that with WT PRMT1. (C) The M155A mutant uses a distributive mechanism to catalyze the formation of ADMA. The large percent turnover of ω-MMA suggests that ω-MMA is released prior to the rebinding in preparation for the second round of methylation.

explanation, which is equally supported by the data, involves the PRMT1-catalyzed reaction being primarily driven by bringing the substrate guanidinium closer to the *S*-methyl group of SAM.

H293 Mutants. H293 has been thought to play the role of a general base by accepting a proton from N_{η_2}; however, this residue is >6 Å from the approximate position of the substrate guanidinium, a distance that is too far to directly remove the proton. Although a water-mediated proton transfer mechanism is possible, the high basicity of the substrate guanidinium makes this mechanism intellectually unsatisfying, and we have suggested (see above) that proton loss could occur prior to, concomitant with, or even after methyl transfer, and that H293 may not act as a general base. To probe this hypothesis, we created the H293Q and H293A mutants. For the H293Q mutant, the k_{cat} is decreased by 41-fold, whereas negligible changes in the K_m values were observed, indicating that the 110- and 125-fold decreases in the k_{cat}/K_m values for AcH4−21 and SAM, respectively, are driven by k_{cat}. For the H293A mutant, the effects on k_{cat}/K_m are similar in magnitude, with the k_{cat}/K_m values for AcH4−21 and SAM decreased by 256- and 50-fold, respectively. Although these results indicate that H293 plays a critical role in catalysis and could be interpreted as being consistent with a role for H293 as the general base, alternative explanations are also possible. For example, in the structure of the PRMT1·SAH complex, H293 appears to form a salt bridge with D51, a conserved residue that is present on αY. Given the short distance between the side chains of H293 and D51 (i.e., 2.6 Å), this interaction likely plays a critical role in forming the two-helix boundary that separates the SAM and peptide binding portions of the active site (Figure 5). As such, one would expect that disruption of this interaction would lead to decreased activity via the inability to properly form the substrate and cofactor binding pockets. This is especially likely when one considers that Y39, H45, M48, and R54 are present on helix αY and αZ and likely play key roles in both PRMT1 catalysis (e.g., Y39 and R54) and formation of the active site cleft (e.g., H45 and M48). Consistent with this possible role for H293 is the fact that the K_i for SAH is increased by 11-fold (Table 4). This is the case because either the alanine or glutamine mutations would not be expected to affect SAM binding, only k_{cat}. Given that R54 is also present on helix αY, some of the effects of mutating this residue may also be due to destabilizing the formation of the PRMT1 substrate and cofactor binding pockets.

dx.doi.org/10.1021/bi102022e |*Biochemistry* 2011, 50, 3332–3345

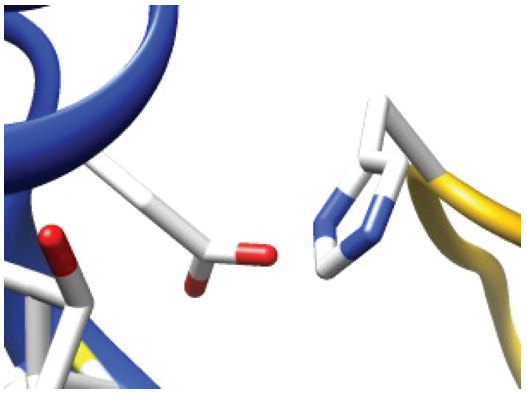

Figure 5. Interaction of D51 and H293. The kinetic effects of the H293 mutations can be explained by the fact that a salt bridge likely forms between D51 and H293, which are separated by only 2.6 Å. A disruption of this interaction could possibly prevent the proper formation of the binding pockets. This figure was prepared with UCSF Chimera using the coordinates for PRMT1 (PDB entry 1ORI).

Y39 Mutant. In CARM1, Y154 appears to be important for both cofactor binding and orienting E267 (Y154 and E267 correspond to Y39 and E153 in PRMT1, respectively[19−21]). Although the Y154F mutant appears to abolish CARM1 activity, this was a single-point assay and only relative rates were measured.[21] Thus, to establish the role of the corresponding residue in PRMT1, we created the Y39F mutant and determined the kinetic parameters. Although this mutation has only small, ∼2-fold effects, on the K_m values for AcH4−21 and SAM, the K_i for SAH is increased by ∼20-fold, thereby confirming that this residue is important for cofactor binding; the lack of a more dramatic effect on the SAM K_m reflects the multistep nature of the reaction, where K_d is not equal to K_m. The importance of this residue was further illustrated by the 20-fold decrease in the k_{cat}/K_m value observed for AcH4−21 and the 20-fold decrease seen with SAM. The position of this residue within the PRMT1 active site and the fact that k_{cat} is decreased by 8.3-fold suggest that this residue may also play an important role in rate enhancement; the specific role of this residue in catalysis is described below (see pH Studies).

S102 Mutants. Given that disruption of the interaction between the S102 hydroxyl and the Y39 backbone carbonyl appears to negatively regulate CARM1,[21] we also investigated the role of S102. For these studies, we generated the S102A and S102E mutants; the latter mutant was generated to mimic constitutively phosphorylated PRMT1. Somewhat surprisingly, the results of these studies indicate that neither mutant negatively impacts the PRMT1 kinetic parameters. The k_{cat}, K_m, and k_{cat}/K_m values are virtually identical to those obtained for the WT enzyme. These results suggest that in contrast to the situation with CARM1, even if this residue is phosphorylated, no effect on PRMT1 activity is likely.

pH Studies. To further improve our understanding of PRMT1 catalysis, pH−rate profiles were generated for the WT enzyme by determining k_{cat} and k_{cat}/K_m values for both SAM and the RGG3 peptide over a pH range of 6.0−9.25. The RGG3 peptide was used in place of the AcH4−21 peptide to simplify the interpretation of the pH−rate profiles. This is the case because this peptide has kinetic parameters comparable to those of the AcH4−21 peptide and, more importantly, because, with the exception of the N-terminus (pK_a ∼ 8.0), this peptide lacks

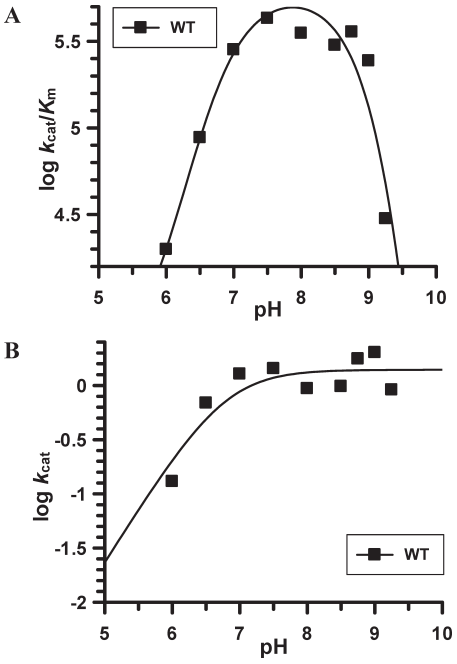

Figure 6. pH profiles of WT PRMT1 with SAM. (A) The log k_{cat}/K_m vs pH plot is used to determine the pK_a of ionizable groups on the enzyme or substrate. (B) The log k_{cat} vs pH plot is used to determine the pK_a of ionizable groups in the ES complex.

residues that typically ionize within the pH range under study. Note that at all pH values enzyme activity was linear with respect to time, indicating that the loss of activity at the pH extremes was not due to a nonspecific effect on enzyme structure. Also note that k_{cat}/K_m is the apparent second-order rate constant for the reaction of free substrate and free enzyme [or when one substrate (A) is saturating, the EA complex], and therefore, the pH dependence of k_{cat}/K_m monitors the ionization state of these entities. In contrast, effects on k_{cat} are interpreted as being due to the presence of important ionizable groups in the enzyme·substrate complex.

With SAM as the varied substrate, the plot of log k_{cat}/K_m versus pH is bell-shaped and is consistent with the presence of two ionizable groups that are important for substrate capture; pK_a values of 6.2 ± 0.3 and 10.5 ± 0.4 were assigned to the ascending and descending limbs, respectively (Figure 6A). With respect to k_{cat}, the rate of the reaction increases with increasing pH until a limiting value is reached (Figure 6B). Fitting the data to eq 4 yields a pK_a value of 5.1 ± 0.8. Although it is difficult to definitively assign an observed pK_a to a particular residue, or functional group on a substrate, the structures of PRMT1, SAM, and the RGG3 peptide suggest several possible residues and/or functional groups whose ionization could alter substrate capture or k_{cat}. With respect to the ascending limb, protonation of the SAM carboxylate (pK_a ∼ 2 in solution), D51, E100, E144, and E153 could explain the loss in activity as the pH decreases. However, most of these groups are readily ruled out. For example, the pK_a of the SAM carboxylate is significantly lower than the pK_a for the ascending limb of the k_{cat}/K_m versus pH−rate profiles, effectively ruling this group out. Consistent with this notion is the fact that the R54A mutation does not affect the K_i for SAM. Although protonation of D51, which is the residue that interacts with H293, could also explain the loss of

activity at low pH, the fact that the pH−rate profiles obtained for the H293A mutant show a similar loss of activity at low pH (vide infra) argues against this possibility. Protonation of E100 could also potentially explain the loss of activity at low pH. However, the fact that little to no effect on the kinetic parameters was observed when this residue was mutated to alanine makes this suggestion unlikely. Of the two remaining residues, i.e., E144 and E153, the residue most likely responsible for the loss of activity at low pH is E153. We surmise that this is the case because the E144Q mutant retains considerable activity; thus, the ionization of this residue would also be expected to minimally impact the reaction rate. In contrast, the activity of the E153Q mutant is significantly decreased and similar to that obtained for the E153A mutant, thereby suggesting that protonation of the E153 carboxylate would have a profound negative impact on rate acceleration. Also consistent with the ionization of this residue corresponding to the ascending limb is the fact that the pK_a of a glutamate residue in solution is typically in the range of 4−5. In total, these data suggest that E153 must be deprotonated for optimal PRMT1 activity.

With respect to the descending limb, deprotonation of the amino group on SAM (pK_a ∼ 9.5 in solution), the N-terminal amino group on the RGG3 peptide (pK_a ∼ 8 in solution), Y39, and H293 could explain the loss in activity as the pH increases. Given the similarities in the pK_a values of these functional groups, it is more difficult to definitively assign the pK_a of the descending limb. Nevertheless, the fact that the pK_a of the N-terminal amine on the RGG3 peptide is significantly lower than the pK_a of the descending limb argues against the notion that the ionization of this group is responsible for the decreased activity at high pH. Note also that the pK_a of an arginine residue is 12.5 and is significantly higher than the pK_a observed for the descending limb, arguing against the idea that ionization of these residues in the RGG3 peptide is responsible for the loss of activity. The fact that the concentration of the RGG3 peptide is fixed in these experiments further argues against these possibilities because, here, k_{cat}/K_m is the second-order rate constant for the reaction of SAM with the E·RGG3 complex, and thus, k_{cat}/K_m monitors the ionization state of these entities, and not the RGG3 peptide. The fact that the calculated pK_a of H293 (7.9) is significantly lower than the pK_a observed for the descending limb suggests that this residue is also not responsible for the loss of activity at high pH. Of the two remaining functional groups or residues, i.e., the amino group on SAM and the Y39 phenol, deprotonation of either one could be responsible for the loss of activity at high pH, as the pK_a values of these groups (i.e., 9.5 and 10.5, respectively) are similar to that obtained for the descending limb.

When the RGG3 peptide is used as the varied substrate, the plot of log k_{cat}/K_m versus pH is also bell-shaped with an ascending limb pK_a of 5.2 ± 0.2 and a descending limb pK_a of 10.0 ± 0.3 (Figure 7A). For the same reasons described above, these pK_a values likely correspond to the protonation states of E153 and Y39, respectively. Note that the assignment of the descending limb to the amino group on SAM can be at least partially ruled out because the concentration of SAM is fixed in these experiments; thus, k_{cat}/K_m is the second-order rate constant for the reaction of the RGG3 peptide with the E·SAM complex, and as such, k_{cat}/K_m monitors the ionization state of these entities, and not SAM. Interestingly, and in contrast to the data presented for SAM, the plot of the log k_{cat} values versus pH is relatively flat, thereby indicating that when the peptide is the varied substrate the turnover number is not influenced by pH (Figure 7B). This

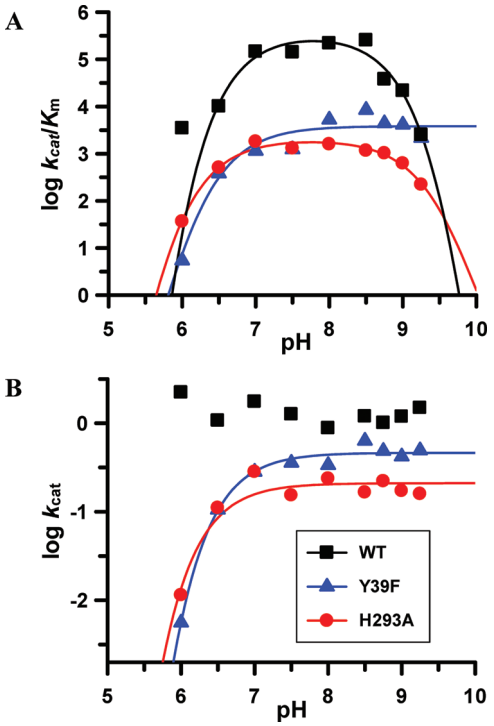

Figure 7. pH profiles of WT PRMT1 and mutants with the RGG3 peptide. (A) The log k_{cat}/K_m vs pH plot is used to determine the pK_a of ionizable groups on the enzyme or substrate. (B) The log k_{cat} vs pH plot is used to determine the pK_a of ionizable groups in the ES complex.

difference most likely reflects a change in the rate-determining step for the reaction. Given that PRMT1 methylates its substrates in a partially processive fashion, these data are most consistent with product release being rate-limiting when the peptide is the varied substrate, as opposed to the case when the concentration of SAM is varied and chemistry, a conformational change, or SAM binding is potentially rate-limiting.

pH−rate profiles were also generated for the H293A and Y39F mutants, using the RGG3 peptide as the varied substrate. Note that we focused on these mutants because of their putative roles as the general base and because the tyrosine residue possesses an ionizable group that potentially corresponds to the basic limb of the WT pH−rate profile. Also note that we generated profiles for only the RGG3 peptide because we envisioned that these data would provide greater insights into the factors that are important for promoting the transfer of methyl groups to the peptide substrate. For the H293A and Y39F mutants, the plots of log k_{cat} versus pH are sigmoidal, with the rates increasing as a function of pH to a limiting value (Figure 7B). Fitting the data to eq 4 identified pK_a values of 4.8 ± 0.4 and 5.1 ± 0.8 for the H293A and Y39F mutants, respectively. Interestingly, these data differ substantially from those obtained with the WT enzyme, where changes in pH did not affect k_{cat}. This difference likely reflects a change in the rate-limiting step. Consistent with this possibility is the fact that the mutation of either residue decreases k_{cat} by ≥11-fold; thus, chemistry is potentially rate-limiting for both the H293A and Y39F mutants. In total, these data indicate that both residues play an important role in rate enhancement.

With respect to k_{cat}/K_m, the plots of log k_{cat}/K_m versus pH for both WT and H293A are similarly bell-shaped, and the pK_a values obtained with the H293A mutant (i.e., 5.2 ± 1.6 and 10.1 ± 0.9)

Table 5. Solvent Isotope Effects (SIEs) and Solvent Viscosity Effects for WT and PRMT1 Mutants

	$^{SIE}k_{cat}$	$^{SVE}k_{cat}$	$^{SIE}k_{cat}/K_m$	$^{SVE}k_{cat}/K_m$
WT	1.0	0.7	0.9	0.9
E144A/E153A	0.8	0.7	0.4	0.6
Y39F	0.4	0.4	0.3	1.8
R54A	1.2	1.3	0.6	1.7
H293A	0.1	1.2	0.1	1.6

are nearly identical to those obtained for the WT enzyme (Figure 7A). Conversely, only the ascending limb is evident in the Y39F k_{cat}/K_m versus pH plot, which suggests that the phenolic side chain of this residue corresponds to the descending limb of the k_{cat}/K_m versus pH−rate profile. These results suggest that Y39 must be protonated for optimal activity and that deprotonation of the phenol leads to a decrease in activity either via the loss of a key hydrogen bond between Y39 and E153 or via electrostatic repulsion between these two residues that leads to a decrease in enzyme activity. In contrast, it is interesting to note that the lack of an effect of mutating H293 on the shape of the pH−rate profiles suggests that the general acid/base properties of this residue are not important for rate enhancement. As such, these data lend support to the idea that H293 does not act as the general base that deprotonates the substrate guanidinium.

Solvent Isotope Effects. To further probe the catalytic mechanism of PRMT1, we also determined the steady state kinetic parameters for the PRMT1-catalyzed reaction in D_2O, using the AcH4−21 peptide as the varied substrate. For these experiments, the rates of the reaction were measured in ≥92% D_2O and compared to those obtained in H_2O at the corresponding pL. For the WT enzyme, a small inverse SIE (0.9) is apparent on k_{cat}/K_m when the peptide is the varied substrate (Table 5 and Table S2 of the Supporting Information). Although this result could be interpreted as being consistent with general base catalysis being unimportant for rate enhancement (a normal SIE would be expected if general base catalysis plays a prominent role in rate enhancement), the fact that chemistry is unlikely to be rate-limiting for the peptide substrate with the wild-type enzyme (see above) could suggest that the lack of an effect is due to the fact that product release is insensitive to the identity of the solvent. Given this possibility, we also determined SIEs for the Y39F, R54A, E144A/E153A, and H293A mutants, because the large decreases in k_{cat} (∼5−20-fold) suggest that chemistry is rate-limiting for these enzymes. To help to confirm this possibility, we examined the processivity of the mutant enzymes described above. The results of these studies (Figure S2 of the Supporting Information) indicated that the Y39F, R54A, E144A/E153A, and H293A mutants do not methylate the AcH4−21 peptide in a partially processive fashion, further suggesting that chemistry is rate-limiting for at least a subset of these mutant enzymes. The change in the k_{cat} versus pH−rate profiles observed for the H293A and Y39F mutants further supports this notion. Note that for the majority of the mutants examined, relatively small inverse SIEs ($^{SIE}k_{cat}$ and $^{SIE}k_{cat}/K_m$ values of ∼0.6−0.9) were observed on both k_{cat} and k_{cat}/K_m (Table 5). The two exceptions are the R54A and H293A mutants. For the R54A mutant, the $^{SIE}k_{cat}$ is small and normal ($^{SIE}k_{cat}$ = 1.2), whereas for the H293A mutant, the SIE on both k_{cat} and k_{cat}/K_m is large and inverse ($^{SIE}k_{cat}$ and $^{SIE}k_{cat}/K_m$ values of 0.1). Note that these experiments were performed in parallel and that representative data from one of at least two independent experiments are reported in Table 5.

Inverse SIEs are often attributed to medium effects, the dissociation of a metal-chelated water, viscosity effects, or effects on thiol ionization.[30] Although medium effects are difficult to exclude, they are typically small and normally ignored.[30] Additionally, the lack of a requirement for metal ions or the presence of a thiol within the active site of PRMT1 suggests that the observed inverse SIE is not due to either of these possibilities. To control for the effect of the increased viscosity of D_2O, the kinetic parameters were determined in the presence of 10% glycerol, a concentration of glycerol that closely mimics the viscosity of D_2O (Table 5 and Table S3 of the Supporting Information). The results of these solvent viscosity experiments (SVEs) indicate that, with the exception of the R54A and H293A mutants, the k_{cat} values for the WT and mutant enzymes were accelerated in the presence of 10% glycerol, suggesting that for these mutants the inverse SIE on k_{cat} can be attributed to a viscosity effect. With respect to k_{cat}/K_m, inverse SVEs were detected for only the WT and the E144A/E153A double mutant, suggesting again that for these mutants the inverse SIE on k_{cat}/K_m can be attributed to a viscosity effect. However, normal SVEs were observed for the Y39F, R54A, and H293A mutants, indicating that the inverse SIEs are due to a direct effect of D_2O on the PRMT1-catalyzed reaction. Although it is difficult to speculate about the molecular basis for the inverse SIEs, there are at least two possible explanations. First, given that deuterium atoms are known to form stronger hydrogen bonds, D_2O may stabilize the structure of PRMT1 and thereby enhance the rate of the reaction. This may be particularly true for the H293A mutant, where a very large, and likely unprecedented, inverse SIE was observed (SIE = 0.1). As mentioned previously, the disruption of the salt bridge between H293 and D51, which would be caused by the alanine mutation, likely prevents the proper formation of the substrate and cofactor binding pockets. However, when the H293A mutant is assayed in D_2O, this solvent stabilizes the structure of PRMT1 and compensates for the loss of the interaction between H293 and D51. As k_{cat}/K_m reports on all steps up to and including the first irreversible step of the reaction, which for PRMT1 is likely methyl transfer, the observed inverse SIEs for the mutant enzymes may, alternatively, be reporting on the formation of the dication intermediate because rehybridization of the ω-nitrogen from sp^2 to sp^3 would be expected to yield an inverse isotope effect. Regardless of the nature of the inverse SIE, the lack of a normal SIE for WT PRMT1, and all of the catalytically impaired mutants, suggests that general base catalysis is unimportant for the PRMT1-catalyzed reaction and, more specifically, suggests that H293 does not act as a general base.

CONCLUSIONS

PRMT1 activity impacts a number of important cell signaling pathways (e.g., gene transcription), and its activity is dysregulated in heart disease and cancer. As such, PRMT1 represents a novel therapeutic target, and we have been focused on developing inhibitors targeting this isozyme.[13−16] To gain insights that could guide the design of inhibitors with increased potency and selectivity, we used a combination of site-directed mutagenesis, pH−rate profiles, and SIEs to begin to characterize the catalytic mechanism of PRMT1. For the mutagenesis studies, we focused our efforts on examining the contribution of eight residues lining the active site pocket of PRMT1, including Y39, R54, E100, S102, E144, E153, M155, and H293, which, on the basis of structures of PRMT family members, have been hypothesized to

be important for SAM binding (i.e., Y39, R54, and E100), the regiospecific generation of ADMA (i.e., M155), the regulation of CARM1 (i.e., S102 and Y39), general base catalysis (i.e., H293), and modulating the nucleophilicity of the substrate guanidinium (i.e., E144 and E153).

The results of the mutagenesis studies indicate that while R54 and E100 form hydrogen bonds and electrostatic interactions with the SAM carboxylate and the ribose moiety, respectively, neither residue is important for SAM binding. However, the fact that the R54 mutations negatively impact the kinetic parameters obtained for the peptide substrate helps to confirm that the observed hydrogen bond or electrostatic interaction between the R54 guanidinium and the E144 carboxylate is important for rate enhancement; this interaction likely orients E144 such that it can properly position N_{η_2} for nucleophilic attack on the *S*-methyl group of SAM. In contrast to R54 and E100, M155 is important for SAM binding, as evidenced by the 26-fold increase in the K_i for SAH when this residue is mutated to alanine. The k_{cat}/K_m obtained for SAM is similarly affected. As M155 forms the bottom of the adenine portion of the SAM binding pocket, the loss of hydrophobic interactions between M155 and the adenine ring, which occurs in the M155L and M155A mutants, likely results in both a loss of affinity and an inability to properly position the cofactor for methyl transfer. M155 is also important for the processivity but not the regiospecificity of the PRMT1-catalyzed reaction; i.e., this residue does not direct the formation of ADMA over SDMA, which has been suggested previously.

E144 and E153 have previously been suggested to orient the substrate guanidinium and modulate its nucleophilicity to promote methyl transfer.[18] Consistent with previous mutagenesis studies that measured only relative rates,[9] our results indicate that both residues are important for PRMT1 catalysis. Interestingly, however, the charge and position of E144 appear to be relatively unimportant for rate enhancement as both the E144D and E144Q mutants retain considerable activity. These results suggest that the hydrogen bond between E144 and the substrate guanidinium is most important, and that this interaction likely orients N_{η_2} for nucleophilic attack on the *S*-methyl group of SAM. In contrast, both the charge and position of E153 are important for rate enhancement, and the results are consistent with the previous suggestion that this residue modulates the nucleophilicity of the guanidinium group by redistributing electron density toward N_{η_1} and N_δ.

With respect to Y39, in addition to being important for SAM binding (because of its position at the top of the SAM binding pocket), this residue appears to be important for rate enhancement. This is apparent from the 20-fold decrease in k_{cat}/K_m when the peptide is the varied substrate. This result suggests that the phenolic hydroxyl group enhances the rate of catalysis. On the basis of structures of PRMT1 family members, this residue likely forms a hydrogen bond with E153, and this interaction is important for positioning the E153 carboxylate such that it can modulate the nucleophilicity of the substrate guanidinium. This hypothesis is supported by the fact that PRMT1 loses activity at high pH, where the deprotonated form of Y39 would be expected to predominate and the resultant electrostatic repulsions between this residue and the E153 carboxylate would lead to a loss of activity. This latter observation is further supported by the loss of the high pK_a when this residue is mutated to phenylalanine.

The results obtained for the H293A mutant are particularly interesting. Although this residue has been suggested to act as general base to deprotonate the substrate guanidinium and thereby enhance the nucleophilicity of this group, our results do not support such a hypothesis. This is the case because effects are observed on both the kinetic parameters determined for SAM and the peptide substrate. Additionally, the pH−rate profiles obtained for the H293A mutant are similar to those obtained for the WT enzyme, which indicates that the ionization of this residue does not contribute to either the rate-limiting step of the reaction or substrate capture, which should encompass the methyl transfer step. Although the contribution of this residue to rate enhancement may not be apparent in the pH−rate profiles, because this residue is unimportant for substrate capture or the rate-limiting step of the reaction, we deem this possibility unlikely and suggest that the decreased activity observed when this residue is mutated is due to the loss of a critical salt bridge between this residue and D51. The loss of this salt bridge would be expected to destabilize the two N-terminal helices and impact cofactor and peptide binding, both of which occur when this residue is mutated. Consistent with this notion is the fact that the K_i for SAH is increased by 11-fold. The notion that H293 is not a general base is consistent with the fact that this residue is ≥6 Å distal from the approximate site of the substrate guanidinium, a distance that is too great for this residue to play such a role.

In total, the data described above support a mechanism in which SAM and a protein, or peptide, substrate bind to the enzyme in a random fashion to form a ternary complex (Figure 2B). E153 then likely redistributes the electron density toward either N_{η_1} or N_δ, or even both, which enhances the nucleophilicity of N_{η_2}. The methyl group of SAM is then transferred to the protonated guanidinium of the substrate arginine to form a dication intermediate. Although such an intermediate is to the best of our knowledge unprecedented, dianionic carboxylate intermediates have been proposed for several enzymes. Rehybridization of the guanidinium destabilizes the dication intermediate, thereby facilitating the loss of the extra proton to water or an unknown general base. While E144 could serve such a role, this seems unlikely when one considers that the effect of mutating this residue to glutamine has an only small impact on k_{cat}/K_m. Further support for the notion that methyl transfer precedes proton transfer comes from the lack of a normal SIE on both the wild-type enzyme and several catalytically impaired mutants for which chemistry is most likely rate-limiting; a normal SIE would be expected if proton abstraction was rate-limiting. Given that Hedstrom and colleagues[31] have noted that arginine residues can act as general bases, and that the pK_a of those residues is potentially modulated by slight structural perturbations to the normally planar guanidinium, we cannot completely rule out the possibility that E144 and E153 depress the pK_a of the substrate arginine and thereby enhance its nucleophilicity, via such a mechanism. However, it is difficult to rationalize such a mechanism with our findings that the E144A/E153A double mutant possesses considerably more activity than either of the single mutations alone. Thus, we favor the mechanism proposed above in which the methyl group is transferred to the protonated guanidinium. In summary, our results suggest that the PRMT1-catalyzed reaction is primarily driven by bringing the substrate and cofactor into the proximity of each other and that the prior deprotontation of the substrate guanidinium is not required for methyl transfer.

■ ASSOCIATED CONTENT

Supporting Information. Supplementary Tables S1−S3 and Figures S1 and S2. This material is available free of charge via the Internet at http://pubs.acs.org.

AUTHOR INFORMATION

Corresponding Author

*Department of Chemistry, The Scripps Research Institute, 130 Scripps Way, Jupiter, FL 33458. Telephone: (561) 228-2860. Fax: (561) 228-2918. E-mail: Pthompso@scripps.edu.

Funding Sources

This work was supported in part by the University of South Carolina Research Foundation and TSRI Scripps Florida (P.R.T.).

ACKNOWLEDGMENT

We thank Raman Parkesh for help with the pK_a calculations.

ABBREVIATIONS

PRMT, protein arginine methyltransferase; SAM, *S*-adenosylmethionine; SAH, *S*-adenosylhomocysteine; ω-MMA, monomethylarginine; ADMA, asymmetrically dimethylated arginine; SDMA, symmetrically dimethylated arginine; NOS, nitric oxide synthase; NO, nitric oxide; ERα, estrogen receptor α; E_2, estrogen; FAK, focal adhesion kinase; PI3K, phosphoinositide 3-kinase; NR, nuclear receptor; AR, androgen receptor; TRIS, tris(hydroxymethylaminomethane); HEPES, 4-(2-hydroxyethyl)-1-piperazineethanesulfonic acid; DTT, dithiothreitol; DMF, dimethylformamide; EDTA, (ethylenedinitrilo)tetraacetic acid; TFA, trifluoroacetic acid; BSA, bovine serum albumin; PDB, Protein Data Bank.

REFERENCES

(1) Bedford, M. T. (2007) Arginine methylation at a glance. *J. Cell Sci. 120*, 4243–4246.

(2) Bedford, M. T., and Clarke, S. G. (2009) Protein arginine methylation in mammals: Who, what, and why. *Mol. Cell 33*, 1–13.

(3) Bedford, M. T., and Richard, S. (2005) Arginine methylation an emerging regulator of protein function. *Mol. Cell 18*, 263–272.

(4) Wolf, S. S. (2009) The protein arginine methyltransferase family: An update about function, new perspectives and the physiological role in humans. *Cell. Mol. Life Sci. 66*, 2109–2121.

(5) Nicholson, T. B., Chen, T., and Richard, S. (2009) The physiological and pathophysiological role of PRMT1-mediated protein arginine methylation. *Pharmacol. Res. 60*, 466–474.

(6) Di Lorenzo, A., and Bedford, M. T. (2010) Histone arginine methylation. *FEBS Lett.*XXX.

(7) Tang, J., Frankel, A., Cook, R. J., Kim, S., Paik, W. K., Williams, K. R., Clarke, S., and Herschman, H. R. (2000) PRMT1 is the predominant type I protein arginine methyltransferase in mammalian cells. *J. Biol. Chem. 275*, 7723–7730.

(8) Herrmann, F., Lee, J., Bedford, M. T., and Fackelmayer, F. O. (2005) Dynamics of human protein arginine methyltransferase 1 (PRMT1) in vivo. *J. Biol. Chem. 280*, 38005–38010.

(9) Zhang, X., and Cheng, X. (2003) Structure of the predominant protein arginine methyltransferase PRMT1 and analysis of its binding to substrate peptides. *Structure 11*, 509–520.

(10) Chen, X., Niroomand, F., Liu, Z., Zankl, A., Katus, H. A., Jahn, L., and Tiefenbacher, C. P. (2006) Expression of nitric oxide related enzymes in coronary heart disease. *Basic Res. Cardiol. 101*, 346–353.

(11) Le Romancer, M., Treilleux, I., Leconte, N., Robin-Lespinasse, Y., Sentis, S., Bouchekioua-Bouzaghou, K., Goddard, S., Gobert-Gosse, S., and Corbo, L. (2008) Regulation of estrogen rapid signaling through arginine methylation by PRMT1. *Mol. Cell 31*, 212–221.

(12) Koh, S. S., Chen, D., Lee, Y. H., and Stallcup, M. R. (2001) Synergistic enhancement of nuclear receptor function by p160 coactivators and two coactivators with protein methyltransferase activities. *J. Biol. Chem. 276*, 1089–1098.

(13) Osborne, T. C., Obianyo, O., Zhang, X., Cheng, X., and Thompson, P. R. (2007) Protein arginine methyltransferase 1: Positively charged residues in substrate peptides distal to the site of methylation are important for substrate binding and catalysis. *Biochemistry 46*, 13370–13381.

(14) Osborne, T., Roska, R. L., Rajski, S. R., and Thompson, P. R. (2008) In situ generation of a bisubstrate analogue for protein arginine methyltransferase 1. *J. Am. Chem. Soc. 130*, 4574–4575.

(15) Obianyo, O., Causey, C. P., Osborne, T. C., Jones, J. E., Lee, Y. H., Stallcup, M. R., and Thompson, P. R. (2010) A chloroacetamidine-based inactivator of protein arginine methyltransferase 1: Design, synthesis, and in vitro and in vivo evaluation. *ChemBioChem 11*, 1219–1223.

(16) Bicker, K. L., Obianyo, O., Rust, H. L., and Thompson, P. R. (2011) A combinatorial approach to characterize the substrate specificity of protein arginine methyltransferase 1. *Mol. BioSyst. 7*, 48–51.

(17) Obianyo, O., Osborne, T. C., and Thompson, P. R. (2008) Kinetic mechanism of protein arginine methyltransferase 1. *Biochemistry 47*, 10420–10427.

(18) Zhang, X., Zhou, L., and Cheng, X. (2000) Crystal structure of the conserved core of protein arginine methyltransferase PRMT3. *EMBO J. 19*, 3509–3519.

(19) Yue, W. W., Hassler, M., Roe, S. M., Thompson-Vale, V., and Pearl, L. H. (2007) Insights into histone code syntax from structural and biochemical studies of CARM1 methyltransferase. *EMBO J. 26*, 4402–4412.

(20) Troffer-Charlier, N., Cura, V., Hassenboehler, P., Moras, D., and Cavarelli, J. (2007) Functional insights from structures of coactivator-associated arginine methyltransferase 1 domains. *EMBO J. 26*, 4391–4401.

(21) Feng, Q., He, B., Jung, S. Y., Song, Y., Qin, J., Tsai, S. Y., Tsai, M. J., and O'Malley, B. W. (2009) Biochemical control of CARM1 enzymatic activity by phosphorylation. *J. Biol. Chem. 284*, 36167–36174.

(22) Branscombe, T. L., Frankel, A., Lee, J. H., Cook, J. R., Yang, Z., Pestka, S., and Clarke, S. (2001) PRMT5 (Janus kinase-binding protein 1) catalyzes the formation of symmetric dimethylarginine residues in proteins. *J. Biol. Chem. 276*, 32971–32976.

(23) Leatherbarrow, R. J. (2004) *GraFit*, version 5.0.11, Erathicus Software, Staines, U.K.

(24) Fisk, J. C., Sayegh, J., Zurita-Lopez, C., Menon, S., Presnyak, V., Clarke, S. G., and Read, L. K. (2009) A type III protein arginine methyltransferase from the protozoan parasite *Trypanosoma brucei*. *J. Biol. Chem. 284*, 11590–11600.

(25) Case, D. A., Cheatham, T. E., III, Darden, T., Gohlke, H., Luo, R., Merz, K. M., Jr., Onufriev, A., Simmerling, C., Wang, B., and Woods, R. J. (2005) The Amber biomolecular simulation programs. *J. Comput. Chem. 26*, 1668–1688.

(26) Bas, D. C., Rogers, D. M., and Jensen, J. H. (2008) Very fast prediction and rationalization of pKa values for protein-ligand complexes. *Proteins 73*, 765–783.

(27) Boehr, D. D., Thompson, P. R., and Wright, G. D. (2001) Molecular mechanism of aminoglycoside antibiotic kinase APH(3′)-IIIa: Roles of conserved active site residues. *J. Biol. Chem. 276*, 23929–23936.

(28) Knuckley, B., Bhatia, M., and Thompson, P. R. (2007) Protein arginine deiminase 4: Evidence for a reverse protonation mechanism. *Biochemistry 46*, 6578–6587.

(29) Troffer-Charlier, N., Cura, V., Hassenboehler, P., Moras, D., and Cavarelli, J. (2007) Expression, purification, crystallization and preliminary crystallographic study of isolated modules of the mouse coactivator-associated arginine methyltransferase 1. *Acta Crystallogr. F63*, 330–333.

(30) Karsten, W. E., Lai, C. J., and Cook, P. F. (1995) Inverse solvent isotope effects in the NAD-malic enzyme reaction are the result of the viscosity difference between D_2O and H_2O: Implications for solvent isotope effect studies. *J. Am. Chem. Soc. 117*, 5914–5918.

(31) Guillen Schlippe, Y. V., and Hedstrom, L. (2005) A twisted base? The role of arginine in enzyme-catalyzed proton abstractions. *Arch. Biochem. Biophys. 433*, 266–278.

Supporting Information

for

Mechanistic Studies on the Transcriptional Coactivator Protein Arginine Methyltransferase 1 †

Heather L. Rust[1,2], Cecilia Zurita-Lopez[3], Steven Clarke[3], and Paul R. Thompson[1,2*]

[1] Department of Chemistry, The Scripps Research Institute, Scripps Florida, 130 Scripps Way, Jupiter, Florida 33458

[2] Department of Chemistry & Biochemistry, University of South Carolina, 631 Sumter Street, Columbia, SC 29208

[3]Department of Chemistry and Biochemistry, University of California, Los Angeles, 607 Charles E. Young Drive East, Los Angeles, CA 90095

Running Title: Catalytic Mechanism of PRMT.

† This work was supported in part by the University Of South Carolina Research Foundation (P.R.T) and TSRI Scripps Florida.

* To whom correspondence should be addressed: Department of Chemistry, The Scripps Research Institute, Scripps Florida, 130 Scripps Way, Jupiter, Fl, 33458 tel: (561)-228-2860; fax: (561)-228-2918; e-mail: Pthompso@scripps.edu.

Table S1. Site-directed Mutagenesis Forward Primers

Mutant	Forward Primer
Y39F	5’-GACTACTACTTTGACTCCTTTGCCCACTTTGGCATCCACG-3’
R54K	5’-GCTAAAGGATGAGGTGAAAACCCTCACGTACC-3’
R54A	5’-GCTAAAGGATGAGGTGGCAACCCTCACGTACC-3’
E100D	5’-GCAAGGTCATTGGGATCGACTGCTCCAGTATCTC-3’
E100Q	5’-GCAAGGTCATTGGGATCCAGTGCTCCAGTATCTC-3’
E100A	5’-GCAAGGTCATTGGGATCGCGTGCTCCAGTATCTC-3’
S102E	5’-GCAAGGTCATTGGGATCGAGTGCGAGAGTATCTCTGATTATGCTGTG-3’
S102A	5’-GCAAGGTCATTGGGATCGAGTGCGCCAGTATCTCTGATTATGCTGTG-3’
E144D*	5’-CATCATCATCAGCGACTGGATGGGCTACTGCC-3’
E144Q*	5’-CATCATCATCA GCCAGTGGATGGGCTACTGCC-3’
E144A	5’-CATCATCATCAGCGCGTGGATGGGTTATTGCC-3’
E153D	5’-GGTTATTGCCTCTTCTATGACTCCATGCTCAACACTGTG-3’
E153Q	5’-GGTTATTGCCTCTTCTATCAGTCCATGCTCAACACTGTG-3’
E153A	5’-GGTTATTGCCTCTTCTATGCGTCCATGCTCAACACTGTG-3’
M155L	5’-CC TCTTCTATGAGTCCCTGCTCAACACTGTGCTGC-3’
M155A	5’-CCTCTTCTATGAGTCCGCGCTCAACACTGTGCTGC-3’
H293Q	5’-GAGTCTCCATACACACAGTGGAAGCAGACTGTG-3’
H293A	5’-CCTGAGTCTCCATACACAGCTTGGAAGCAGACTGTG-3’

*hPRMT1 sequence

Table S2. Solvent Isotope Effect (SIE): Kinetic parameters for WT and PRMT1 mutants determined in H_2O and D_2O

Mutant	K_m (μM)	k_{cat} (min^{-1})	$^{SIE}k_{cat}$	k_{cat}/K_m ($M^{-1}\cdot min^{-1}$)	$^{SIE}k_{cat}/K_m$
WT[a]	1.1 ± 0.5	$4.6 \times 10^{-1} \pm 2 \times 10^{-2}$		4.1×10^{5}	
WT[b]	1.0 ± 0.5	$4.5 \times 10^{-1} \pm 1 \times 10^{-2}$	1.0	4.6×10^{5}	0.9
E144A/E153A[a]	3.0 ± 0.7	$1.32 \times 10^{-1} \pm 4 \times 10^{-3}$		4.4×10^{4}	
E144A/E153A[b]	1.4 ± 0.7	$1.60 \times 10^{-1} \pm 6 \times 10^{-3}$	0.8	1.1×10^{5}	0.4
Y39F[a]	2.0 ± 0.7	$4.2 \times 10^{-2} \pm 2 \times 10^{-3}$		2.1×10^{4}	
Y39F[b]	1 ± 2	$9.9 \times 10^{-2} \pm 4 \times 10^{-3}$	0.4	6.9×10^{4}	0.3
R54A[a]	5 ± 1	$6.0 \times 10^{-2} \pm 3 \times 10^{-3}$		1.3×10^{4}	
R54A[b]	2.3 ± 0.8	$5.2 \times 10^{-2} \pm 2 \times 10^{-3}$	1.2	2.3×10^{4}	0.6
H293A[a]	11.1 ± 0.6	$1.81 \times 10^{-2} \pm 2 \times 10^{-4}$		1.6×10^{3}	
H293A[b]	9 ± 3	$2.2 \times 10^{-1} \pm 2 \times 10^{-2}$	0.1	2.4×10^{4}	0.1

[a]H_2O. [b]D_2O.

Table S3. Solvent Viscosity Effects (SVE): Kinetic parameters determined in H_2O and 10% Glycerol

Mutant	K_m (μM)	k_{cat} (min^{-1})	$^{SVE}k_{cat}$	k_{cat}/K_m ($M^{-1}\cdot min^{-1}$)	$^{SVE}k_{cat}/K_m$
WT[a]	1.1 ± 0.5	$4.6 \times 10^{-1} \pm 2 \times 10^{-2}$		4.1×10^{5}	
WT[b]	1.4 ± 0.3	$6.7 \times 10^{-1} \pm 1 \times 10^{-2}$	0.7	4.6×10^{5}	0.9
E144A/E153A[a]	3.0 ± 0.7	$1.32 \times 10^{-1} \pm 4 \times 10^{-3}$		4.4×10^{4}	
E144A/E153A[b]	2.9 ± 0.3	$1.99 \times 10^{-1} \pm 2 \times 10^{-3}$	0.7	6.9×10^{4}	0.6
Y39F[a]	2.0 ± 0.7	$4.2 \times 10^{-2} \pm 2 \times 10^{-3}$		2.1×10^{4}	
Y39F[b]	9 ± 1	$1.03 \times 10^{-1} \pm 2 \times 10^{-3}$	0.4	1.2×10^{4}	1.8
R54A[a]	5 ± 1	$6.0 \times 10^{-2} \pm 3 \times 10^{-3}$		1.3×10^{4}	
R54A[b]	6 ± 1	$4.8 \times 10^{-2} \pm 1 \times 10^{-3}$	1.3	7.7×10^{3}	1.7
H293A[a]	11.1 ± 0.6	$1.81 \times 10^{-2} \pm 2 \times 10^{-4}$		1.6×10^{3}	
H293A[b]	16 ± 3	$1.51 \times 10^{-2} \pm 5 \times 10^{-4}$	1.2	9.7×10^{2}	1.6

[a]H_2O. [b]10% Glycerol.

Figure S1

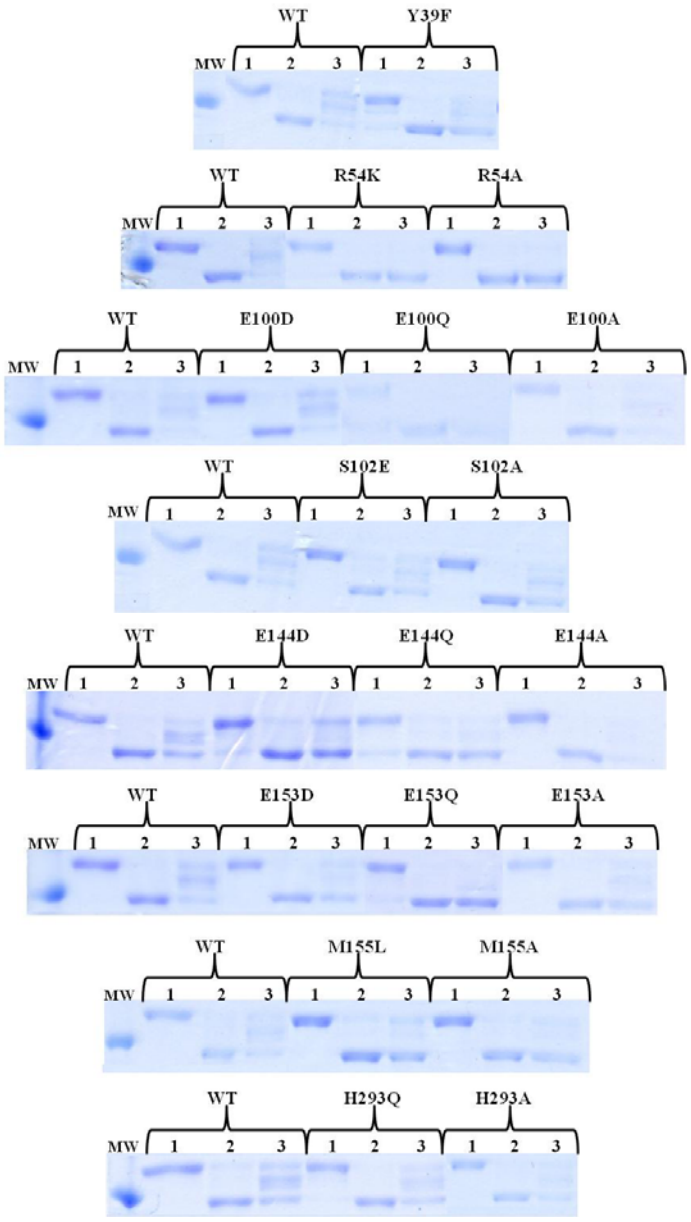

Figure S1. Partial Proteolysis of PRMT1 mutants. WT and PRMT1 mutants (5 μg) were incubated in the absence and presence of subtilisin (0.75 μg/mL final) (Lanes 1 & 2). WT and PRMT1 mutants were also incubated with SAH (500 μM) in the presence of subtilisin (Lane 3).

Figure S2

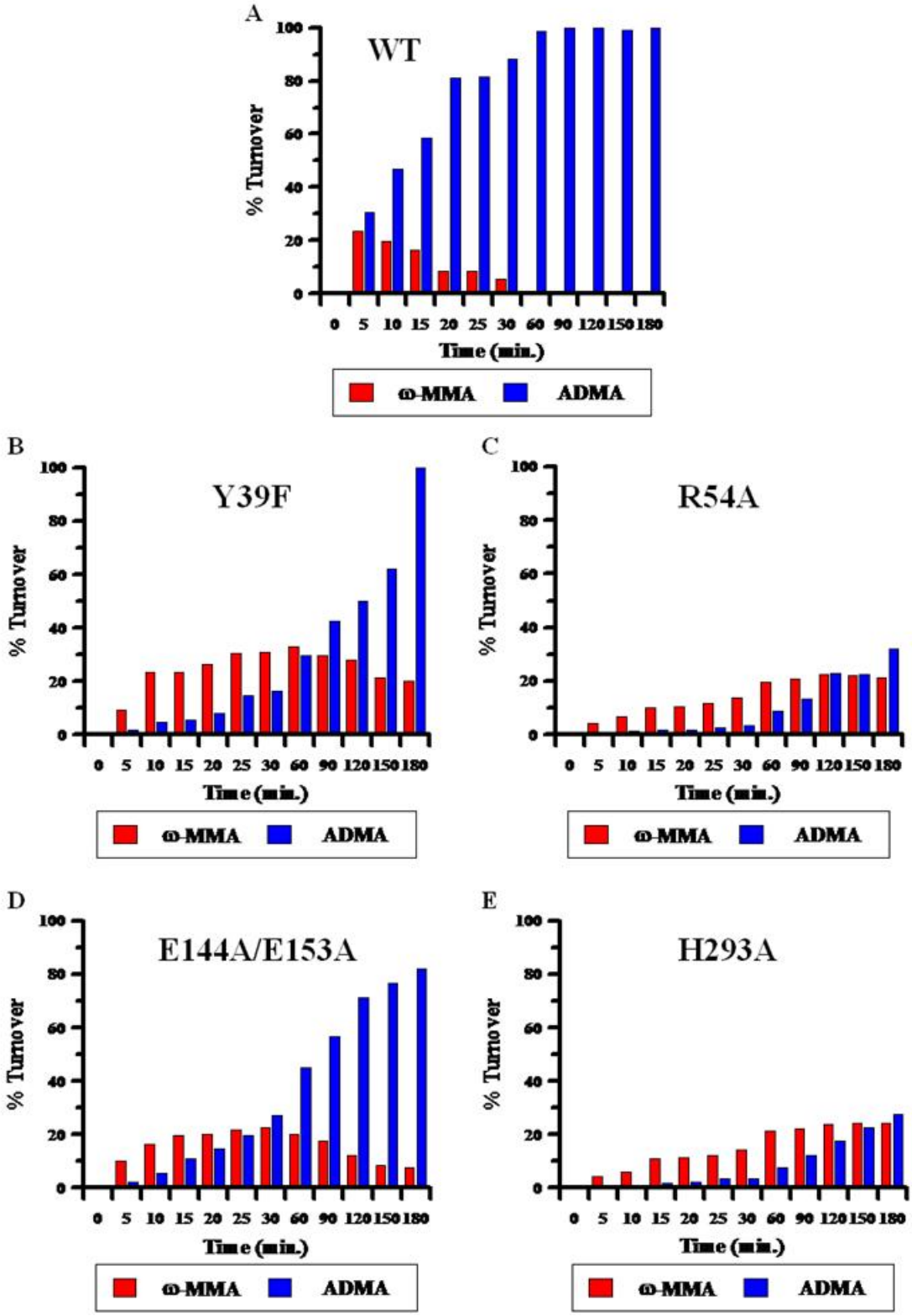
A
WT
% Turnover
Time (min.)
0 5 10 15 20 25 30 60 90 120 150 180
ω-MMA
ADMA
B
Y39F
C
R54A
D
E144A/E153A
E
H293A

Figure S2. Processivity of WT PRMT1 and mutants. (A) WT PRMT1 uses a partially processive mechanism to catalyze the formation of ADMA. (B) TheY39F mutant uses a distributive mechanism to catalyze the formation of ADMA in which ω-MMA is released prior to the rebinding in preparation for the second round of methylation. (C) The R54A mutant also utilizes a distributive mechanism. (D) The E144A/E153A mutant uses a partially processive mechanism, however, the formation of ADMA is slower than WT. (E) H293A uses a distributive mechanism to catalyze the formation of ADMA.